EXPERIMENTATION AND MODELLING OF OXIDE CONDUCTING FUEL CELL WORKING ON INDUSTRIAL WASTE

A Final Year Project Report

Presented to

SCHOOL OF MECHANICAL & MANUFACTURING ENGINEERING

Department of Mechanical Engineering

NUST

ISLAMABAD, PAKISTAN

In Partial Fulfillment
of the Requirements for the Degree of
Bachelors of Mechanical Engineering

---

by

Fahd Rehman
Muhammad Ahsan
Usama Rehman
Muhammad Khizar

EXAMINATION COMMITTEE

We hereby recommend that the final year project report prepared under our supervision by:

Fahd Rehman	Reg. no. 123155
Muhammad Ahsan	Reg. no. 122328
Usama Rehman	Reg. no. 111733
Muhmmad Khizar	Reg. no. 128105

Titled: "EXPERIMENTION AND MODELLING OF OXIDE CONDUCTING FUEL CELL WORKING ON INDUSTRIAL WASTE" be accepted in partial fulfillment of the requirements for the award of DEGREE NAME degree with grade ___

Supervisor: Hafiz Abdur-Rehman, Lecturer, NUST	Dated:
Committee Member: Dr. Emad uddin , HOD SMME, NUST	Dated:
Committee Member: Dr. Rehan Zahid, Assistant Professor, NUST	Dated:

_____ _____

(Head of Department) (Date)

COUNTERSIGNED

Dated: _____ _____

(Dean / Principal

ABSTRACT

The use of conventional energy conversion devices like internal combustion engines and batteries has certain disadvantages including higher emissions of greenhouse gases (which are a threat to the environment contributing to global warming), lower efficiencies and decreasing output with the passage of time in case of batteries. These disadvantages compelled man to look for alternative energy conversion devices, which can replace the internal combustion engines and batteries. One such device is a fuel cell, it is an electrochemical device, which converts the chemical energy of a fuel directly into electrical energy. The emissions from a fuel cell are significantly less as compared to conventional devices. Fuel cells produce less noise due to no moving parts, give constant output that does not decay over time and promise higher efficiency. The solid oxide fuel cell (SOFC) is a high temperature fuel cell that operates between 600-1000 °C and uses a solid ceramic as an electrolyte. The operation at higher temperature allows the use of cheap catalysts, fuel flexibility and higher reaction rates. This report presents the working of a solid oxide fuel cell, operating at low temperature (500-600 °C) along with a complete mathematical model and computational fluid dynamics analysis of SOFC using COMSOL multi physics software.

ACKNOWLEDGMENTS

Firstly, we would like to acknowledge and thank our supervisor Sir Abdul Rehman for his continuous guidance throughout this work. We would also like to thank Dr.Emad uddin for helping us with the CFD analysis. We appreciate the efforts of Dr. Taki Mehran who guided us through the design phase and Dr. Rizwan Raza who let us use his state of the art fuel cell laboratory. Finally, we would like to thank Sir Zohaib who helped us a lot in the testing of fuel cell.

ORIGINALITY REPORT

FYP Report

ORIGINALITY REPORT

15%	7%	7%	13%
SIMILARITY INDEX	INTERNET SOURCES	PUBLICATIONS	STUDENT PAPERS

PRIMARY SOURCES

1	Submitted to University of Newcastle upon Tyne Student Paper	1%
2	Ni, M.. "Parametric study of solid oxide fuel cell performance", Energy Conversion and Management, 200705 Publication	1%
3	Submitted to Higher Education Commission Pakistan Student Paper	1%
4	Submitted to University College London Student Paper	1%
5	repository.ntu.edu.sg Internet Source	<1%
6	Submitted to University of Ulsan Student Paper	<1%
7	Meng Ni, Michael K.H. Leung, Dennis Y.C. Leung. "Parametric study of solid oxide fuel cell performance", Energy Conversion and	<1%

	Management, 2007 Publication	
8	scholarbank.nus.edu.sg Internet Source	<1%
9	Submitted to Chulalongkorn University Student Paper	<1%
10	Submitted to Ohio University Student Paper	<1%
11	vdocuments.mx Internet Source	<1%
12	Submitted to Engineers Australia Student Paper	<1%
13	Submitted to Imperial College of Science, Technology and Medicine Student Paper	<1%
14	Submitted to Napier University Student Paper	<1%
15	Submitted to Kingston University Student Paper	<1%
16	link.springer.com Internet Source	<1%
17	Submitted to Mae Fah Luang University Student Paper	<1%
18	elib.uni-stuttgart.de	

	Internet Source	<1%
19	Submitted to Brunel University Student Paper	<1%
20	Ibrahim Dincer, Marc A. Rosen, Maan Al-Zareer. "3.10 Electrochemical Energy Production", Elsevier BV, 2018 Publication	<1%
21	www.coursehero.com Internet Source	<1%
22	Submitted to UC, San Diego Student Paper	<1%
23	Submitted to University of Sheffield Student Paper	<1%
24	www.oatext.com Internet Source	<1%
25	Ni, M.. "A modeling study on concentration overpotentials of a reversible solid oxide fuel cell", Journal of Power Sources, 20061207 Publication	<1%
26	Submitted to American University of Beirut Student Paper	<1%
27	Submitted to K12 Incorporated Student Paper	<1%

28	Submitted to Bishop Fenwick High School Student Paper	<1%
29	Submitted to The University of the South Pacific Student Paper	<1%
30	pt.scribd.com Internet Source	<1%
31	eprints-phd.biblio.unitn.it Internet Source	<1%
32	V. Kumaran. "Josiah Willard Gibbs", Resonance, 2007 Publication	<1%
33	epdf.tips Internet Source	<1%
34	Submitted to Universiti Teknologi MARA Student Paper	<1%
35	Wright, S.E.. "Comparison of the theoretical performance potential of fuel cells and heat engines", Renewable Energy, 200402 Publication	<1%
36	www.et.teiath.gr Internet Source	<1%
37	ecommons.usask.ca Internet Source	<1%

Table of Contents

LIST OF TABLES

LIST OF FIGURES

ABBREVIATIONS

SOFC	Solid Oxide Fuel Cell
PAFC	Phosphoric Acid Fuel Cell
PEMFC	Polymer Electrolyte Membrane Fuel Cell
MCFC	Molten Carbonate Fuel Cell
AFC	Alkaline Fuel Cell
LNCZ	Lithium Nickel Copper Zinc

NOMENCLATURE

P_i	Partial Pressure of the specie i where i = CH_4, O_2, H_2
E_0	Reversible Potential
ΔG^0	Change in Gibbs free energy at standard conditions
ε	Porosity of electrode
D_P	Pore size
D_s	Grain size
k_a	Coefficient for exchange current density of the anode
$E_{act,a}$	Activation energy levels at the anode

CHAPTER 1: INTRODUCTION

Problem Identification:

Due to overpopulation and a huge gap between supply and demand, it is the need of the hour that we should devise innovative and efficient ways to use natural resources so that we have a minimum wastage and a lesser damage to the environment. Our country has been facing energy shortage crisis for more than a decade now. Keeping both of the above-mentioned points in mind, we should effectively utilize our natural resources in an eco-friendly way to overcome energy shortage in our country.

Motivation:

Renewable energy sources are the future of energy sector. Scientists and researchers are trying to shift our energy conversion techniques from conventional pollution causing devices to such devices which are less harmful to environment or do not cause any pollution at all.

Photovoltaic cell which harnesses solar energy from sun and converts it to electricity has proven to be an eco-friendly device. Nevertheless, it has some drawbacks. Firstly, its installation is costly. Secondly, it does not give constant output voltage. Moreover, it cannot be installed at every place.

Wind turbine is another pollution free energy converting device. But it has some demerits as well. Wind turbines cannot be installed everywhere. They can be a threat to bird life.

In Pakistan, coal power plants are producing most of the electrical energy. The coal power plants are very reliable. They operate 24/7 with very little downtime. Again, these plants are not so efficient and a threat to environment. The efficiency of coal power plants is nearly 30%.

Internal combustion engines use fossil fuel but their efficiency is low and they emit harmful gases into the environment. In portable applications like locomotives, they are being replaced by batteries. But batteries have their own issues. Batteries need to be recharged and recharging takes time. They cannot provide us with constant voltage. They have low power densities.

Fuel cells have an efficiency of about 70-80%. They consume lesser fuel. They are environment friendly.

Our motivation was to design a fuel cell that operates at a temperature ranging from 500-600°C.

Aim:

"Development and testing of a solid oxide fuel cell that operates at temperatures lower than those of conventional SOFCs."

Objectives:

- CFD analysis and simulation
- Fabrication and Prototype Development
- Testing the prototype and deducing results
- Documentations and Publications

CHAPTER 2: LITERATURE REVIEW

A major portion of energy of the world is produced from coal. Nearly 40% of the power generation in the world is from coal [1]. In terms of contribution to world's power generation, coal stands on second place and soon it will replace oil which is at the top of the list [1]. Globally, the reserves of coal are reported to be 891,531 million tonnes [2]. It is estimated that by the end of the year 2042, the only source of primary energy left in the world would be coal [3].

Pakistan is a country, which has been blessed with huge coal reserves. Pakistan has approximately 186 billion tonnes of coal reserves [4].

Comparison of Carbon Based SOFC and Coal Power Plant

The efficiency of coal power plant is approximately 33% [5]. On the other hand, direct carbon fuel cell has an efficiency of approximately 80% [6]. Fuel cell emits residual gases in lower quantity and at lower rate as compared to the coal power plant [7]. Theoretical fuel usage in case of fuel cell is 100%.

Comparison of Fuel Cells and Batteries

Fuel cells are able to give constant voltage provided that, they are fed with continuous supply of fuel. But, batteries are unable to do so. Fuel cells have higher current densities than batteries [8].

Brief History of Fuel Cell

In 1801, Humphry Davy gave the idea of fuel cell. Christian Friedrich Schönbein made the first fuel cell in 1838. In 1839, Sir William Robert Grove made a fuel cell. This fuel cell was called 'Grove Cell'. The Grove Cell had a zinc anode immersed in dilute H_2SO_4 and a platinum cathode immersed in concentrated nitric acid. Its output voltage was about

1.9 V and powered early American Telegraph system. The Grove cell looked like the one shown in figure 1.

Figure 1. Grove Cell

In 1889, Ludwig Mond and Charles Langer worked on a fuel cell which operated on coal gas and air. William White Jaques was the first researcher who used Phosphoric acid in the electrolyte bath. In the 1920s, a research was carried out in Germany which led to the development of SOFCs. In 1932, Francis T Bacon contributed to the development of fuel cells. Before Bacon, Platinum electrodes and Sulfuric acid were used. Bacon introduced the use of nickel electrodes and alkaline electrolyte. In 1959, Bacon Cell had a voltage of five-kilowatt and could power a welding machine. In October 1959, Harry Karl Ihrig engineered a 20 horsepower tractor which was powered by a fuel cell. Meanwhile, US Air Force started to use Fuel cell in their vehicle. In NASA's space programs Gemini and Apollo, fuel cells were used both for power generation and for producing drinkable water. Fuel cells also found their way into space programs of Russia. General Motors

developed first fuel cell car in 1966. This car was given the name Chevrolet Electrovan. The car could go as fast as up to 70 mph with a range of 120 miles and had a PEM fuel cell. In 1990s, California, an official order was given to find alternative ways to power the vehicles. Meanwhile, fuel cells were set out to be employed in portable devices like phones and laptops [9].

Fuel Cell Types

Based on the type of electrolyte, fuel cells can be divided into five groups, which are Phosphoric Acid Fuel Cell (PAFC), Solid-Oxide Fuel Cell (SOFC), Polymer Electrolyte Membrane Fuel Cell (PEMFC), Molten Carbonate Fuel Cell (MCFC), and Alkaline Fuel Cell (AFC) [8]. Their properties are shown in table 1.

Table 1. Description of Major Fuel Cell Types [8]

	PEMFC	PAFC	AFC	MCFC	SOFC
Electrolyte	**Polymer Membrane**	**Liquid H_3PO_4 (immobilized)**	**Liquid KOH (immobilized)**	**Molten Carbonate**	**Ceramic**
Charge carrier	**H^+**	**H^+**	**OH^-**	**CO_3^{2-}**	**O^{2-}**
Operating Temperature	**80ºC**	**200 ºC**	**60-220 ºC**	**650 ºC**	**600-1000 ºC**
Catalyst	**Platinum**	**Platinum**	**Platinum**	**Nickel**	**Perovskites (ceramic)**
Cell Components	**Carbon based**	**Carbon based**	**Carbon based**	**Stainless based**	**Ceramic based**
Fuel Compatibility	**H_2, methanol**	**H_2**	**H_2**	**H_2, CH_4**	**H_2, CH_4, CO**

Polymer Electrolyte Membrane Fuel Cell:

The Polymer Electrolyte Membrane Fuel Cell (PEMFC) is also known as Solid Polymer Fuel Cell and Proton Exchange Membrane Fuel Cell. In this type of fuel cell, the electrolyte is a polymer membrane. On either side of membrane, anode and cathode are bonded. Such assembly is given the name membrane electrode assembly that can be placed between the flow field plates (bipolar plates) to make a system called "stack". The

working of polymer electrolyte membrane fuel cell is almost identical to that of an acid electrolyte fuel cell since both have H^+ as charge carrier [10].

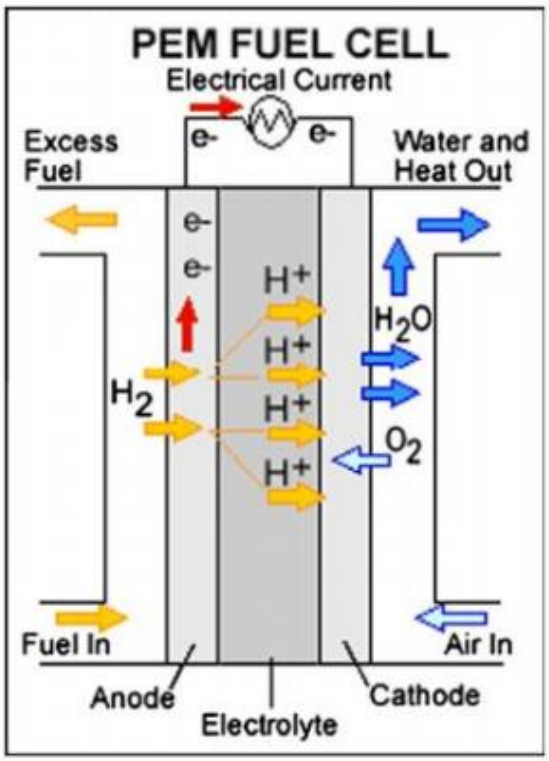

Figure 2. PEM Fuel Cell [11]

At Anode:

$$H_2 \rightarrow 2H^+ + 2e^- \qquad (1)$$

At Cathode:

$$\frac{1}{2}\,O_2 + 2H^+ + 2e^- \rightarrow H_2O \qquad (2)$$

Overall Reaction:

$$H_2 + \frac{1}{2} O_2 \rightarrow H_2O \qquad (3)$$

PEMFCs are not so widely used since they are expensive. In 2009, a PEMFC was manufactured at a cost of about $ 61. It was used in transportation field where its life was registered to be 2500 hours. If cost is not the point of consideration, PEMFCs are better than internal combustion engines [11]. The major drawback associated with PEMFCs is that, they operate at low temperature and hence do not produce enough heat for endothermic reformation [10].

Phosphoric Acid Fuel Cell

In this fuel cell, liquid H_3PO_4 is used as an electrolyte. Here, the charge carrier is a proton. Protons travel through electrolyte while the external circuit acts as a pathway for electrons. Air is delivered at the cathode while hydrogen fuel at the anode.

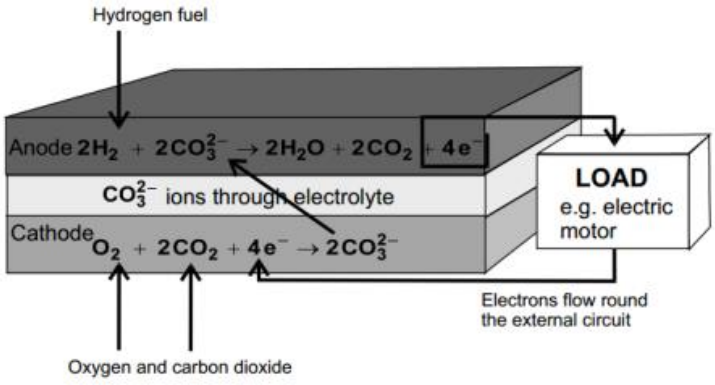

Figure 3. Phosphoric Acid fuel cell [14]

At Anode:

$$\boldsymbol{H_2 \rightarrow 2H^+ + 2e^-} \qquad \textbf{(4)}$$

At Cathode:

$$\boldsymbol{\frac{1}{2}\ O_2 + 2H^+ + 2e^- \rightarrow H_2O} \qquad \textbf{(5)}$$

Overall Reaction:

$$\boldsymbol{H_2 + \frac{1}{2}\ O_2 \rightarrow \quad H_2O} \qquad \textbf{(6)}$$

Since, PAFC does not operate at high temperature; its performance is badly affected by CO. At low temperature, Platinum catalyst is used but this catalyst is degraded by carbon monoxide. Platinum catalyst is supported by using carbon and graphite. The fuel cell's performance is restricted as carbon and graphite are used during the reaction. The operational voltage value should be less than 0.8V to prevent any sort of corrosion [12].

There is also a drawback of using carbon with platinum. Carbon covers the upper surface of Platinum and hence decreases the active surface area.

Alkaline Fuel Cell:

In this type of fuel cell, the electrolyte employed is aqueous KOH. The concentration of KOH solution is around 30% [13]. In AFC, the reaction rates are high, so we can also use non-noble metal electro-catalysts. Two layered structure electrodes are used. One layer is active electro-catalyst layer and the other is a hydrophobic layer.

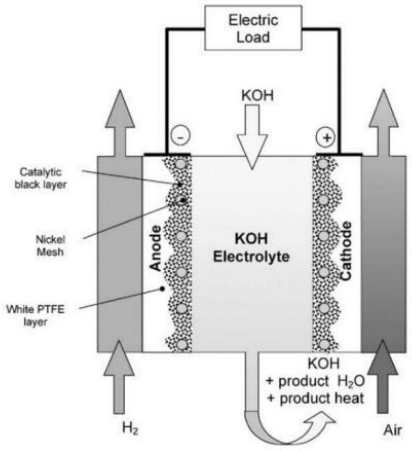

Figure 4. Alkaline Fuel Cell [15]

At Anode:

$$\mathbf{2H_2 + 4OH^- \rightarrow 4H_2O + 4e^-} \qquad \mathbf{(7)}$$

At cathode:

$$\mathbf{O_2 + 2H_2O + 4e^- \rightarrow 4OH^-} \qquad \mathbf{(8)}$$

Overall Reaction:

$$\mathbf{2H_2 + O_2 \rightarrow H_2O} \qquad \mathbf{(9)}$$

The performance of alkaline fuel cell drops with the production of CO_2. So, the performance of AFC is limited if we use hydrocarbons as fuel [16].

Molten Carbonate Fuel Cell:

Here, the reaction takes place between H_2 and O_2 resulting in H_2O. The raw fuel is CH_4 and by a process called 'steam reforming' it is converted into H_2 gas. The process of steam reforming takes place at a high temperature. This is one of the reasons why MCFCs operate at high temperatures. In MCFC, lithiated NiO is used as cathode. It can

dissolve in electrolyte and hence undergo transportation, reduction and precipitation in electrolyte matrix. This can be considered as a drawback of using lithiated NiO as cathode [18].

At Anode:

$$\mathbf{H_2} + \boldsymbol{CO_3^{-2}} \rightarrow \boldsymbol{H_2O} + \mathbf{CO_2} + \mathbf{2}\boldsymbol{e^-} \qquad \textbf{(10)}$$

At Cathode:

$$\frac{\mathbf{1}}{\mathbf{2}}\,\mathbf{O_2} + \mathbf{CO_2} + \mathbf{2e^-} \rightarrow \boldsymbol{CO_3^{-2}} \qquad \textbf{(11)}$$

Overall Reaction:

$$\mathbf{H_2} + \frac{\mathbf{1}}{\mathbf{2}}\,\mathbf{O_2} \rightarrow \boldsymbol{H_2O} \qquad \textbf{(12)}$$

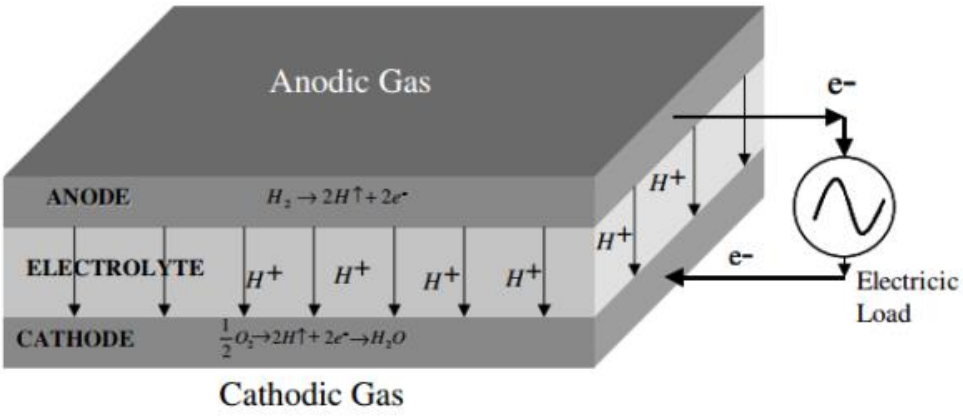

Figure 5. Molten Carbonate Fuel Cell [17]

Solid Oxide Fuel Cell:

The electrode is of a solid ceramic material. Oxygen is converted to O^{2-} ion at cathode. It then passes through electrolyte and reaches anode, where it reacts with CO to produce CO_2.

At Anode:

$$\mathbf{CO + O^{2-} \rightarrow CO_2 + 2e^{-}} \qquad \textbf{(13)}$$

At Cathode:

$$\boldsymbol{O_2 + 4e^{-} \rightarrow 2O^{2-}} \qquad \textbf{(14)}$$

Overall Reaction:

$$\mathbf{CO + O_2 \rightarrow CO_2} \qquad \textbf{(15)}$$

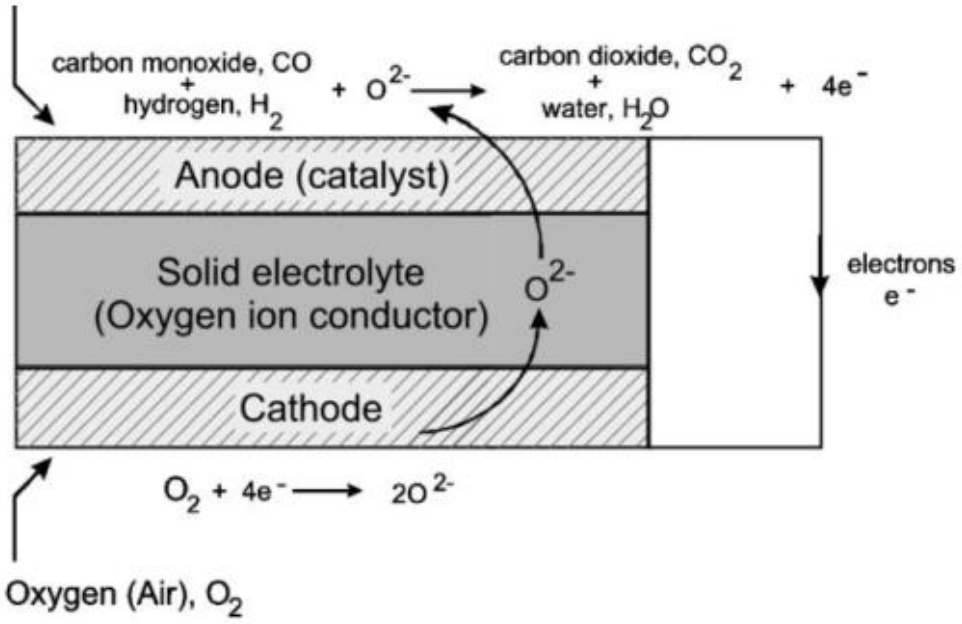

Figure 6. SOFC [19]

The operating temperature of SOFCs is high and hence they could be used in cogeneration. The main components of a fuel cell are cathode, anode and electrolyte or more simply a membrane electrode assembly (MEA). The reduction and oxidation reactions occur at cathode and anode respectively. The electrolyte conducts the ions. The oxygen undergoes reduction at cathode while at anode carbon monoxide undergoes oxidation and converts to carbon dioxide CO_2. The basic sketch of a fuel cell is shown in figure 8.

Figure 7. Basic sketch of a fuel cell showing the reactants and product of the reaction

The reactions occurring within a fuel cell with carbon monoxide as a fuel are shown in figure 8.

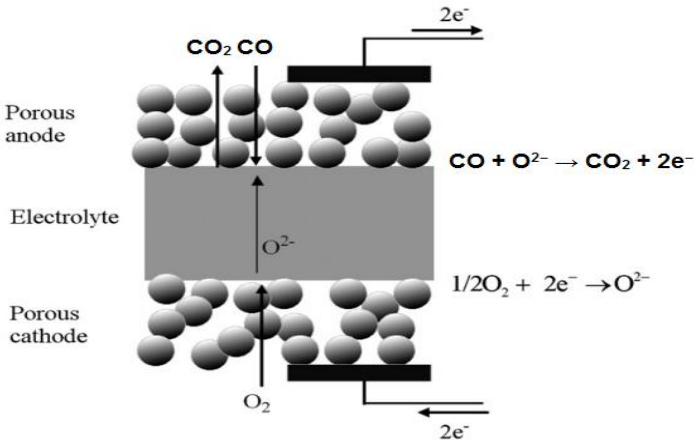

Figure 8. Reactions within a fuel cell along with the basic elements (anode, cathode and electrolyte)

Electrochemical Model:

Some mathematical models have been given to characterize SOFCs, to calculate their over-potentials and the relation of these different types of losses with fuel cell electrolyte thickness and electrode material [20-22]. In all of these studies, it was assumed that exchange current density does not depend upon geometric and operational parameters.

In some studies, concentration over-potential was considered to be negligibly small since SOFCs operate at high temperature [23, 24, 25, and 26]. There were some studies where concentration over-potential was considered to be independent of both geometric and operational parameters [28,29]. Some of the studies considered an overall resistance of fuel cell and there was no clear differentiation between three kinds of over-potentials. [30]

All of the above mentioned models were ambiguous. The reference no. [27] gives a complete electrochemical model with validity. The same model is given in the book. [8]

CHAPTER 3: METHODOLOGY

Material Selection

The latest work being done in the field of SOFCs is to reduce their operating temperature. The material was selected such that the resulting fuel cell operates at 500-600 °C. For this purpose, the following materials were selected for electrodes and electrolyte:

Table 2. Fuel Cell Components Ratio

Component	Thickness Ratio
Anode	0.45
Electrolyte	0.25
Cathode	0.35

Composition

Composition of Electrodes:

Since the fuel cell is symmetric, the composition of cathode and anode is the same. The electrodes are the homogeneous mixture of the following elements:

Table 3. Composition of Electrodes

Elements	Percentage by Molar Mass(%)
Li	12
Ni	24
Cu	14
Zn	32

Role of Each Element in Electrode:

The electrode needs to be porous, should be both ionic and electronic conductor and should also facilitate reaction.

- Li is for ionic conduction
- Cu is for electronic conduction
- Ni acts as a catalyst
- Zn acts as a base phase, provides porosity, facilitates decomposition of fuel and keeps material stable.

Composition of Electrolyte:

The electrolyte is the homogeneous mixture of the following materials:

Table 4. Composition of Electrolyte

Material	**Percentage by Molar Mass(%)**
La	10
Ba	10
CeO	80

Role of Different Materials in Electrolyte

The electrolyte should be dense, electronic insulator and ionic conductor.

- La gives Mechanical Strength
- Ba gives chemical stability
- CeO gives ionic conductivity

Material Synthesis

Material Synthesis for Electrolyte

Method: Co-Precipitation (Since, the electrolyte should be denser)

Steps:

- Take Lanthanum nitrate ($La(NO_3)_3$), Barium Nitrate ($Ba(NO_3)_2$) and Cerium Nitrate ($Ce(NO_3)_3$). Dissolve them in deionize water and make homogeneous solution by stirring.
- Select a precipitating agent. (Since, the solution contains nitrates, the precipitating agent should be a carbonate). Sodium carbonate (Na_2CO_3) is selected as a precipitating agent.
- Add precipitating agent into the solution with continuous stirring. The precipitates will start to settle at the bottom.
- Continue to add deionize water with constant stirring to wash off carbonates.
- Filter the mixture.
- Take the agglomerate in a petri dish and put the petri dish in an oven to dry out moisture.
- Once dried, grind the material.
- Sinter the ground material and grind the resulting material to obtain a homogeneous material.
- Material for electrolyte is ready.

Material Synthesis for Electrode

Steps:

- Take Lithium carbonate (Li_2CO_3), Nickel carbonate ($NiCO_3$), Copper carbonate ($CuCO_3$) and Zinc Nitrate ($Zn(NO_3)_2$).
- Grind these materials in mortar and pestle.
- Take the powder in a petri dish and put it in an oven to dry out moisture
- Once dried, sinter the material.
- Material for electrodes is ready.

Fuel Cell Testing:

The fuel cell was operated at different temperatures and graph of power density vs current density were obtained corresponding to those temperatures.

The fuel cell was operated with hydrogen (H_2) and methane (CH_4) and optimum temperatures for their operations were obtained.

Apparatus:

- Fuel Source
- Air/Oxygen Source
- Flow meters
- DC electronic load
- Pressure Gauges
- Jig for Fuel Cell
- Furnace
- Connecting pipes
- Fuel cell

Figure 9 Fuel Cell Testing Apparatus

Basic Equation for The Output Voltage:

The output voltage of a fuel cell differs by a certain amount from the thermodynamically reversible voltage due to the losses associated with a fuel cell namely the activation losses, concentration losses and Ohmic losses which are later discussed in detail. The basic equation for the voltage output of a fuel cell at a particular current density can be written as follows:

$$V = E - \eta_{act,\,a} - \eta_{act,\,c} - \eta_{conc,\,a} - \eta_{conc,\,c} - \eta_{ohmic} \quad \textbf{(16)}$$

Where:

V = Output Voltage

E = Equilibrium Voltage

η_{act} = Activation Over-potential

η_{conc} = Concentration Over-potential

η_{ohmic} = Ohmic Over-potential

For the equilibrium voltage, Nernst equation is used which is as follows:

$$E = E^{o} + \frac{RT}{2F} ln \left(\frac{[P_{H_2}][P_{O_2}]^{\frac{1}{2}}}{[P_{H_2O}]} \right) \quad \textbf{(17)}$$

Where:

R = ideal gas constant = 8.3145 J mol^{-1} K^{-1}

F = faradays constant = 9.6485 x 10^4 C mol^{-1}

T = Absolute Temperature

P_i = Partial Pressure of the specie i where i = H_2, O_2, H_2O

E_0 = Reversible Potential

E^0 can be calculated using the concept of Gibbs free energy.

$E^0 = -\Delta G^0/nF$

Where:

n = number of moles of electrons taking part in the reaction

ΔG^0 = Change in Gibbs free energy at the standard conditions

Gibbs Free Energy:

The maximum amount of useful work that can be extracted from a system is called Gibbs free energy.

The change in Gibbs free energy at standard conditions can be calculated using the following equation:

$$\Delta G^0 = \Delta H^0 - T\Delta S^0 \qquad (18)$$

Where:

ΔH^0 = Enthalpy of Formation of Product – Enthalpy of formation of Reactants (standard conditions)

ΔS^0 = Entropy difference between reactants and product/s at standard conditions

The values of ΔH^0 and ΔS^0 for the reactants and product of the solid oxide fuel cell working on Hydrogen as a fuel are mentioned in the following table [31]

Table 5. Enthalpy of Formation and Entropy of Reactants and Products

Substance	**ΔH°** **(Enthalpy of Formation)** **kJ/mole**	**S^0 (Entropy)** **J/mole K**
H_2	0	130.68

H_2O(g)	-241.83	188.84
O_2	0	205.00

The related calculations for reversible potential and then the equilibrium voltage are shown in appendix 1. After the necessary calculations, the equilibrium voltage for the fuel cell is given as;

$$\mathbf{E = 1.4664 - 4.476 \times 10^{-4} T - 3.362182128 \times 10^{-5}\ T\ ln\left(\frac{[P_{H_2}]}{[P_{H_2O}]}\right)} \qquad \textbf{(19)}$$

Activation Over-Potential:

For a reaction to proceed in a certain direction (reverse or forward) there is always a barrier/energetic hurdle associated with a reaction which the reactants should overcome before converting into product/s in case of a forward reaction or vice versa. This activation barrier/energetic hurdle gives rise to the activation over-potential which tends to decrease the thermodynamically reversible potential of a fuel cell.

The electrode activation over-potential and current density are related by the Butler-Volmer equation which is as follows:

$$\boldsymbol{J = J_0\left[exp\left(\frac{\alpha n F \eta_{act}}{RT}\right) - exp\left(-\frac{(1-\alpha) n F \eta_{act}}{RT}\right)\right]} \qquad \textbf{(20)}$$

Where:

J = Current Density

J_0 = Exchange Current Density

n = Number of electrons involved per reaction

α = Symmetrical factor

The problem with the Butler-Volmer equation is that it is an implicit equation and to solve an implicit equation involving many unknowns we have to make certain assumptions for the values of variables which may yield impractical results and overall it is quite a tedious task. To get an explicit equation symmetrical factor α is set to be 0.5 [32], [33], [34] after which we may obtain the following explicit equation [35]:

$$\eta_{act,i} = \frac{RT}{F}\, ln\left[\frac{J}{2J_{0,i}} + \sqrt{\left(\frac{J}{2J_{0,i}}\right)^2 + 1}\right] \quad i = Anode, Cathode \qquad (21)$$

Exchange current density at anode or cathode $J_{0,i}$ is an indicator of the readiness of an electrode to undergo a chemical reaction and is very important parameter as activation over-potential depends heavily on it. The value of $J_{0,i}$ is dependent on electrode microstructure properties such as porosity, pore size, temperature, pressure and composition of gases at which a fuel cell operates [36], [37], [38], [39], [40].

Exchange Current Density at Anode:

The expression for the exchange current density at anode can be written as:

$$J_{0,a} = k_a \frac{72X[D_P - (D_P + D_S)\varepsilon]\varepsilon}{D_S^2 D_P^2\left(1-\sqrt{1-X^2}\right)} \times \left(\frac{P_{H_2}}{P_{ref}}\right)\left(\frac{P_{H_2O}}{P_{ref}}\right) exp\left(-\frac{E_{act,a}}{RT}\right) \qquad (22)$$

Where:

ε = Porosity of electrode

D_P = Pore size

D_S = Grain size

X = Ratio of the length of the grain contact neck to grain size

k_a = Coefficient for exchange current density of the anode

$E_{act,a}$ = Activation energy at the anode

Exchange Current Density at Cathode:

The expression for the exchange current density at cathode can be written as:

$$\boldsymbol{J_{0,c} = k_c \frac{72X[D_P-(D_P+D_S)\varepsilon]\varepsilon}{D_S^2 D_P^2\left(1-\sqrt{1-\alpha^2}\right)} \times \left(\frac{P_{O_2}}{P_{ref}}\right)^{0.25} exp\left(-\frac{E_{act,c}}{RT}\right)} \quad \textbf{(23)}$$

Where:

k_c = Coefficient for exchange current density at the cathode

$E_{act,c}$ = Activation energy at the cathode

Concentration Over-Potential:

The resistance to transport of reactants approaching the reaction site and products leaving the reaction site is the reason behind concentration over-potentials. For a SOFC, the concentration over-potentials can be indicated in terms of the gas concentration difference between the electrode surface and the electrode-electrolyte interface which can be written for anode and cathode respectively as:

$$\eta_{conc,a} = \frac{RT}{2F} ln \left(\frac{P^I_{H_2} P_{H_2O}}{P_{H_2} P^I_{H_2O}} \right) \quad \textbf{(24)}$$

$$\eta_{conc,c} = \frac{RT}{2F} ln \left[\left(\frac{P^I_{O_2}}{P_{O_2}} \right)^{\frac{1}{2}} \right] \quad \textbf{(25)}$$

Where:

P^I = Partial pressures at the electrode–electrolyte interface

Partial Pressures at The Electrode–Electrolyte Interface:

Due to the porous structure of electrodes the transportation of gas is carried out by phenomenon of diffusion and hence Fick's model is a convenient tool for determining the interfacial partial pressures. After utilization of which the resulting concentration over-potentials for anode and cathode can be written as [32], [33], [41]:

$$\eta_{conc,a} = \frac{RT}{2F} ln \left(\frac{1 + \frac{RTd_aJ}{2FD_a^{eff} P^0_{H_2O}}}{1 - \frac{RTd_aJ}{2FD_a^{eff} P^0_{H_2}}} \right) \quad \textbf{(26)}$$

$$\eta_{conc,c} = \frac{RT}{4F} ln \left[\frac{P^0_{O_2}}{\frac{P_c}{\delta_{O_2}} - \left(\frac{P_c}{\delta_{O_2}} - P^0_{O_2} \right) exp\left(\frac{RTd_cJ\delta_{O_2}}{4FD_c^{eff} P_c} \right)} \right] \quad \textbf{(27)}$$

Where:

P_c = Operating pressure at the cathode

d_a = Thickness of the anode

d_c = Thickness of the cathode

D_a^{eff} = Effective diffusion coefficient at the anode

D_c^{eff} = Effective diffusion coefficient at the cathode

$$\boldsymbol{\delta_{O_2}} = \frac{\boldsymbol{D_{O_{2,k}}^{eff}}}{\boldsymbol{D_{O_{2,k}}^{eff}} + \boldsymbol{D_c^{eff}}} \quad \textbf{(28)}$$

$D_{O_{2,k}}^{eff}$= Effective Knudsen diffusion coefficient of oxygen

Effective diffusion coefficient

For porous structures there are two types of diffusions which are Knudsen diffusion and molecular diffusion. Molecular diffusion is due to the molecule-molecule interaction while Knudsen diffusion accounts for the molecule-pore wall interaction. The effective diffusion coefficient can be found from the Bosanquet formula [34], [41],[42],[43]:

$$\frac{\boldsymbol{1}}{\boldsymbol{D_a^{eff}}} = \frac{\boldsymbol{\tau}}{\boldsymbol{\varepsilon}}\left(\frac{\boldsymbol{1}}{\boldsymbol{D_{H_2-H_2O}}} + \frac{\boldsymbol{1}}{\boldsymbol{D_{H_2,k}}}\right) \quad \textbf{(29)}$$

$$\frac{\boldsymbol{1}}{\boldsymbol{D_c^{eff}}} = \frac{\boldsymbol{\tau}}{\boldsymbol{\varepsilon}}\left(\frac{\boldsymbol{1}}{\boldsymbol{D_{O_2-N_2}}} + \frac{\boldsymbol{1}}{\boldsymbol{D_{O_2,k}}}\right) \quad \textbf{(30)}$$

Where:

τ = Tortuosity (property to describe fluid flow in porous medium)

$\frac{\varepsilon}{\tau} D_{H_2-H_2O}$ = Effective molecular diffusion coefficient

$\frac{\varepsilon}{\tau} D_{O_2-N_2}$ = Effective molecular diffusion coefficient

$D_{H_2,k}$ = Effective Knudsen diffusion coefficient for H_2

$D_{O_2,k}$ = Effective Knudsen diffusion coefficient for O_2

The molecular diffusion coefficient is determined from kinetic molecular theory while Knudsen diffusion coefficient is found from the Chapman-Enskog theory [34], [41], [42], [43].

Ohmic Over-Potential:

The resistance offered to flow of ions and electrons by the electrodes and electrolyte results in the Ohmic over-potential. The electrical conductivities of connecting plates, anode and cathode are comparably much greater than the electrolyte so we can neglect their contribution to the ohmic over-potential [34], [44]. Then using Ohm's law, we can simplify it as follows:

$$\eta_{ohmic} = \mathbf{2.99 \times 10^{-11}} JLexp\left(\frac{10300}{T}\right) \quad \textbf{(31)}$$

Where:

L = Thickness of electrolyte in micrometers.

Methodology for CFD using COMSOL

At the anode, hydrogen is used as fuel and at the cathode, humidified air, consisting of oxygen, nitrogen and water vapor, is supplied into the inlet. The material transport is described by Maxwell-Stefan's diffusion and convection equations.

At the walls, boundary conditions of the gas channel and Gas diffusion electrode have the insulating condition (zero mass flux). We specify the composition at the inlet, while at the outlet, a convection flux condition is specified. Perpendicular to the boundary, convective term dominates the transport. Continuity equation for mass balance is applied along all the interfaces.

Next to solve the velocity field and the pressure, Brinkman Equations interface was used. To govern the flow velocity in porous Gas diffusion electrodes Brinkman equations are used. To govern the flow in open channels we use compressible Navier-Stokes equations.

A slight overpressure was applied at inlet so that the flow can be driven. Finally, Reacting flow Multiphysics nodes were used to define the couplings between net sinks and sources, velocity and pressure.

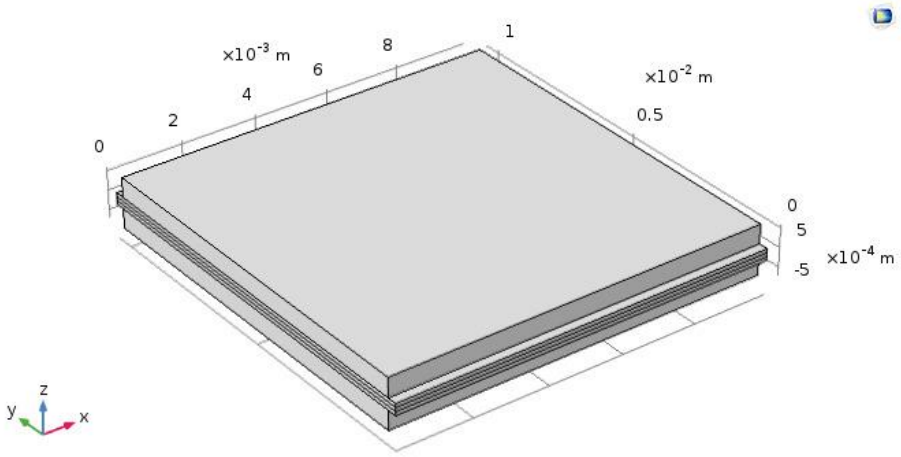

Figure 10. CAD Model of a Single SOFC cell

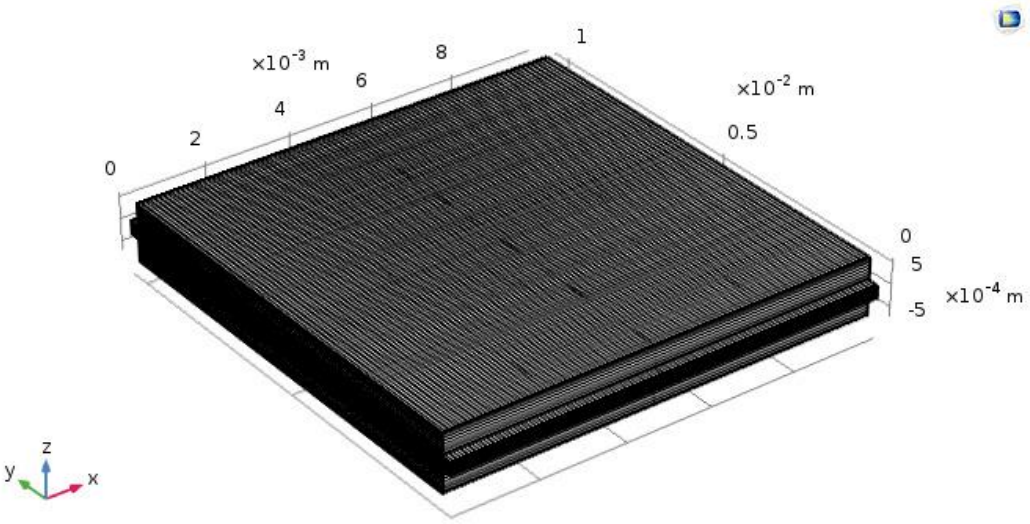

Figure 11. After Mesh Generation

The mesh consisted of 6.392 x 10^3 elements and 1.3 x 10^4 mesh vertices. The average mesh quality was 1.0

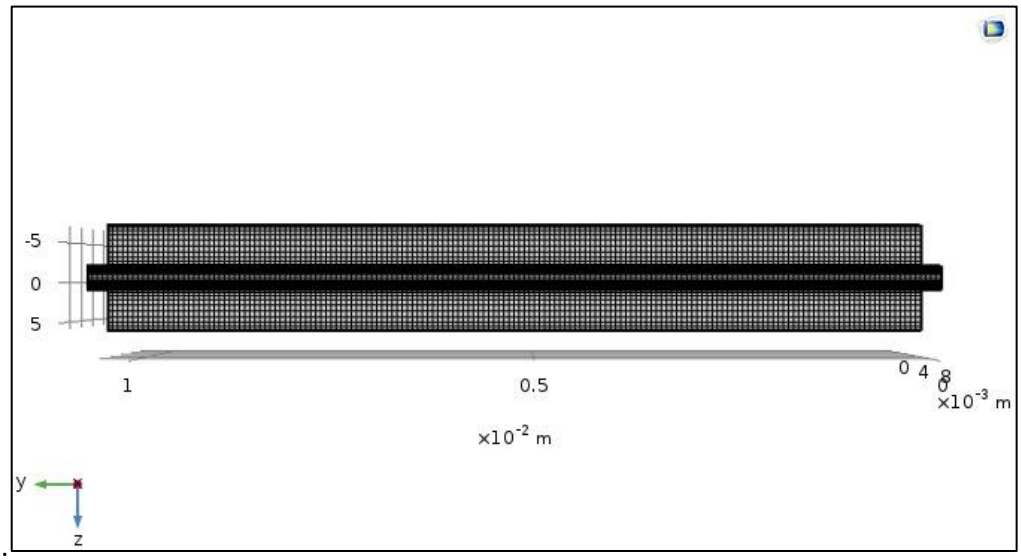

Figure 12. Mesh Front Plane

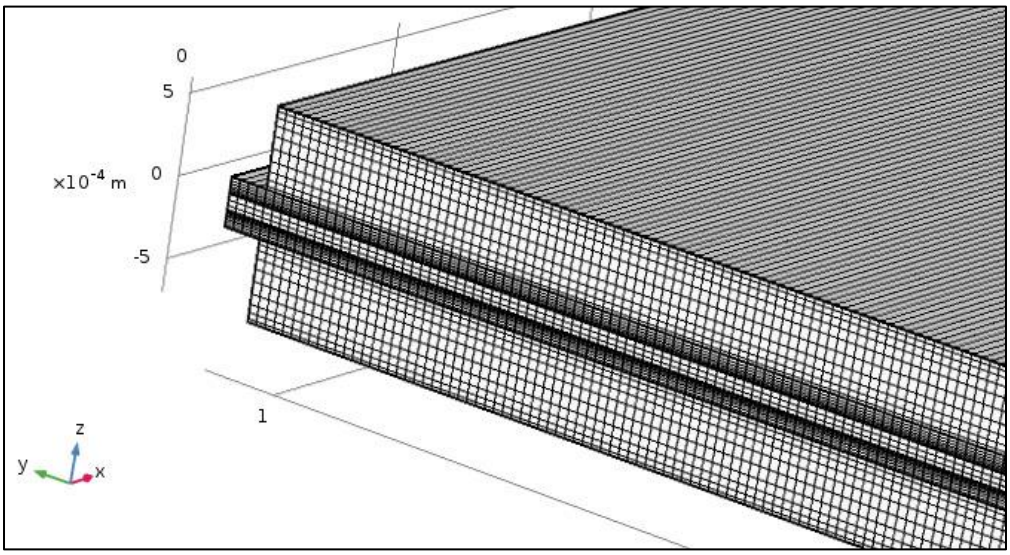

Figure 13. Mesh (zoomed in)

CHAPTER 4: RESULTS and DISCUSSIONS

Analytical Results:

For Hydrogen as Fuel

Equivalent Voltage:

Equivalent voltage depends on two major parameters, which are as under;

- Temperature
- Pressure of hydrogen gas

Effect of Temperature:

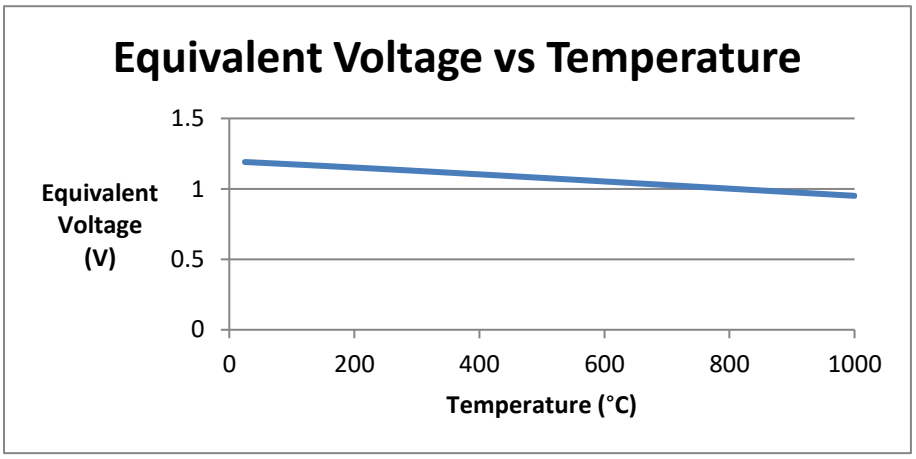

Figure 14. Graph Between Equivalent Voltage and Temperature (Appendix 1)

The conclusion drawn from the graph is that, the equivalent voltage decreases with the increase in temperature hence; there exists an inverse relation between equivalent voltage and temperature. The straight line indicates the liner relation between equivalent voltage and temperature. Note: The above graph is obtained at 1 ATM air pressure and 3.45 atm hydrogen pressure.

Effect of Hydrogen Pressure:

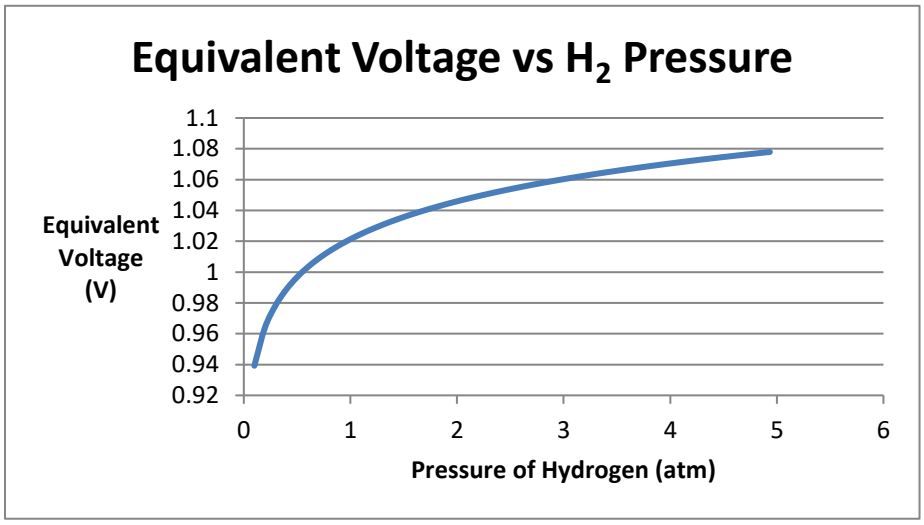

Figure 15. Graph Between Equivalent Voltage and H_2 Pressure (Appendix 2)

Here, the equivalent voltage increases with the increase in the pressure of hydrogen gas. The graph is not linear in nature. The above graph is drawn at 550 °C**.**

Activation Losses:

Activation losses depend on four parameters, which are as under;

- Temperature
- Current Density
- Porosity
- Pore Size

Effect of Temperature:

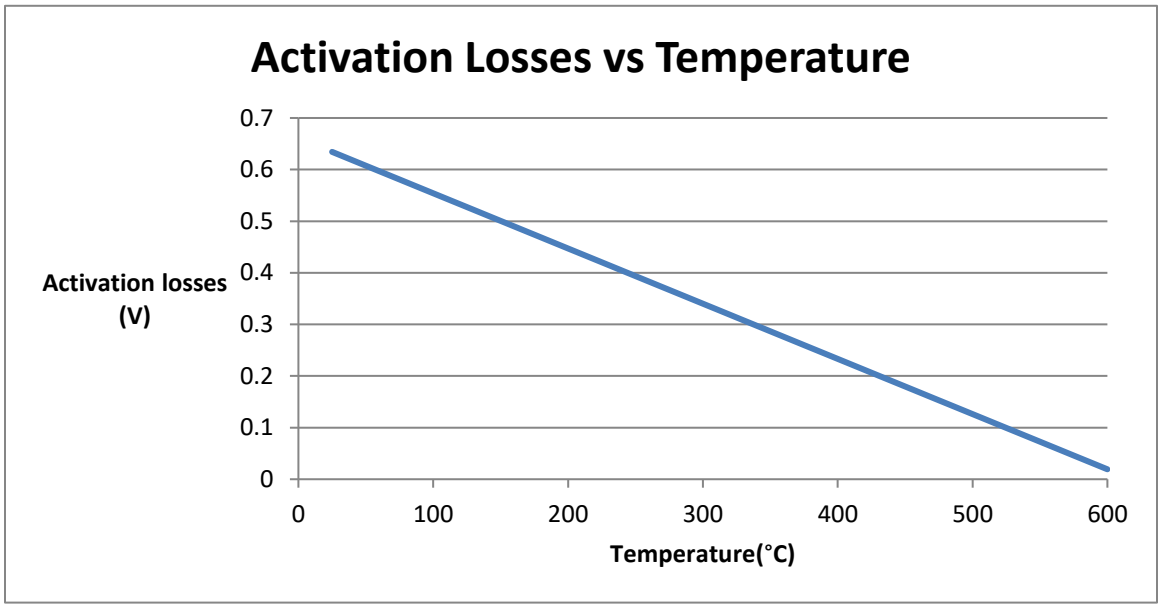

Figure 16. Graph Between Activation Losses and Temperature (Appendix 3)

The conclusion drawn from the graph is that, the activation losses decrease with the increase in temperature hence the reaction can be proceeded easily at a temperature range of 500-600 °C with little activation losses.

Effect of Current Density:

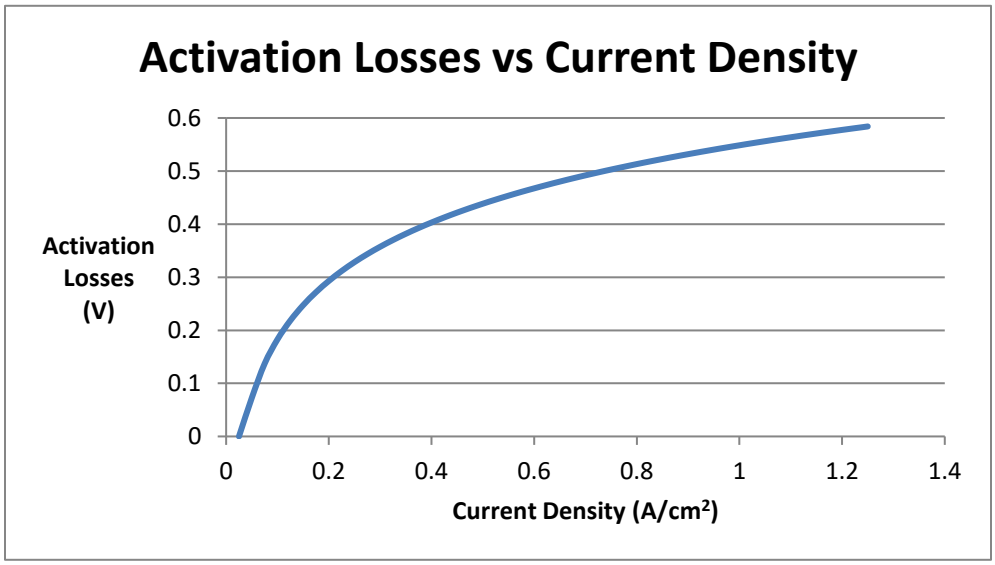

Figure 17. Graph Between Activation Losses and Current Density (Appendix 4)

Here, the activation losses increase with the increase in current density and the increase is not linear but abrupt as evident from the graph.

Effect of Porosity:

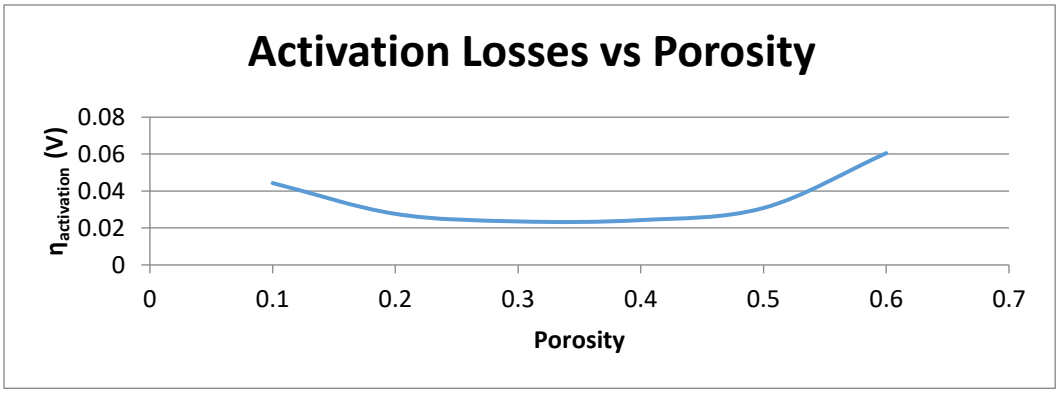

Figure 18. Graph Between Activation Losses and Porosity (Appendix 5)

With an increase in the porosity, the activation over-potential decreases, reaches a minimum at a porosity of around 0.35 and then increases again.

Effect of Pore Size:

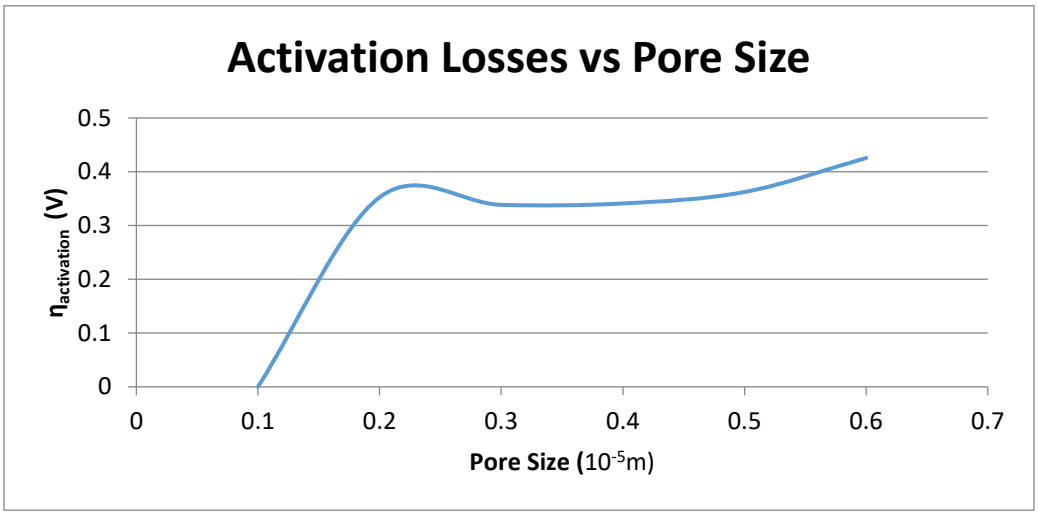

Figure 19. Graph Between Activation Losses and Pore Size (Appendix 6)

Activation over-potential increases, up to a pore size of around 2 μm and then remains approximately constant from 2-5 μm.

Concentration Losses:

There are two types of concentration losses i.e.

- Anode Concentration Losses
- Cathode Concentration Losses

Anode Concentration Losses:

Anode Concentration losses depend on the following two parameters;

- Temperature
- Porosity

Effect of Temperature:

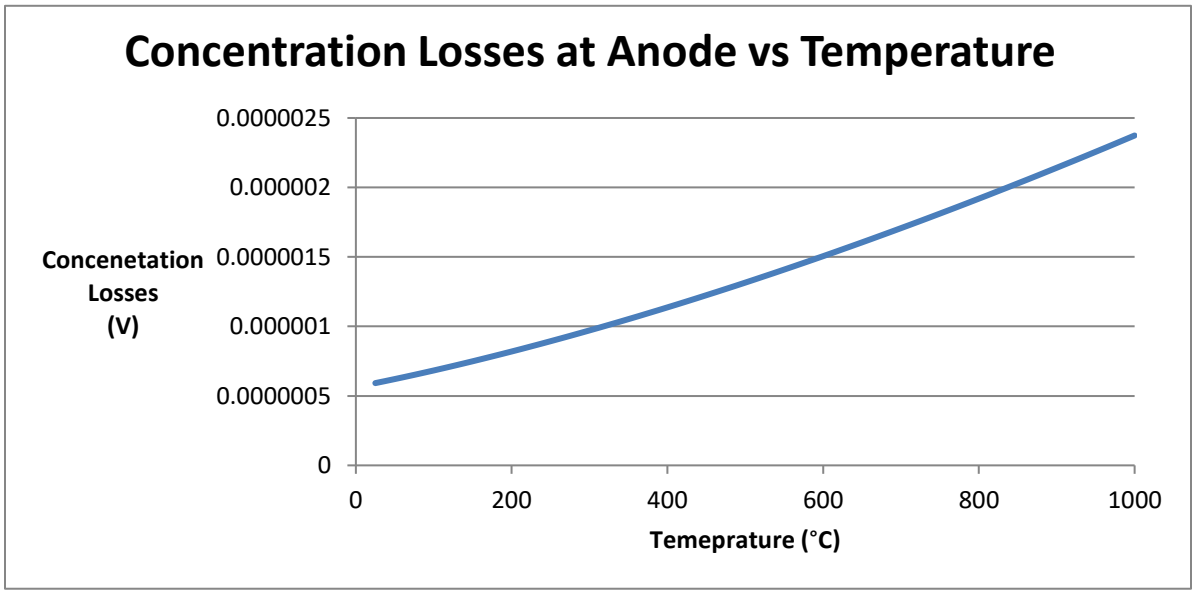

Figure 20. Graph Between Concentration Losses at Anode and Temperature (Appendix 7)

Here, the concentration losses increase with the temperature so we have to optimize the temperature to keep the loss minimum.

Effect of Porosity:

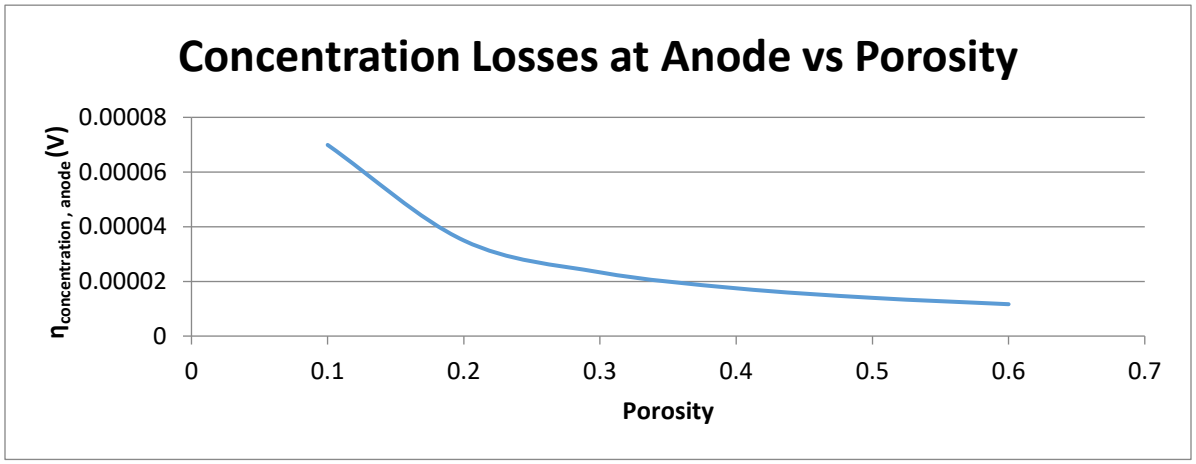

Figure 21. Graph Between Concentration Losses at Anode and Porosity (Appendix 8)

With an increase in porosity, concentration over-potential at anode decreases at a decreasing rate.

Cathode Concentration Losses:

Cathode concentration losses depend on the following parameters;

- Temperature
- Current Density
- Porosity

Effect of Temperature:

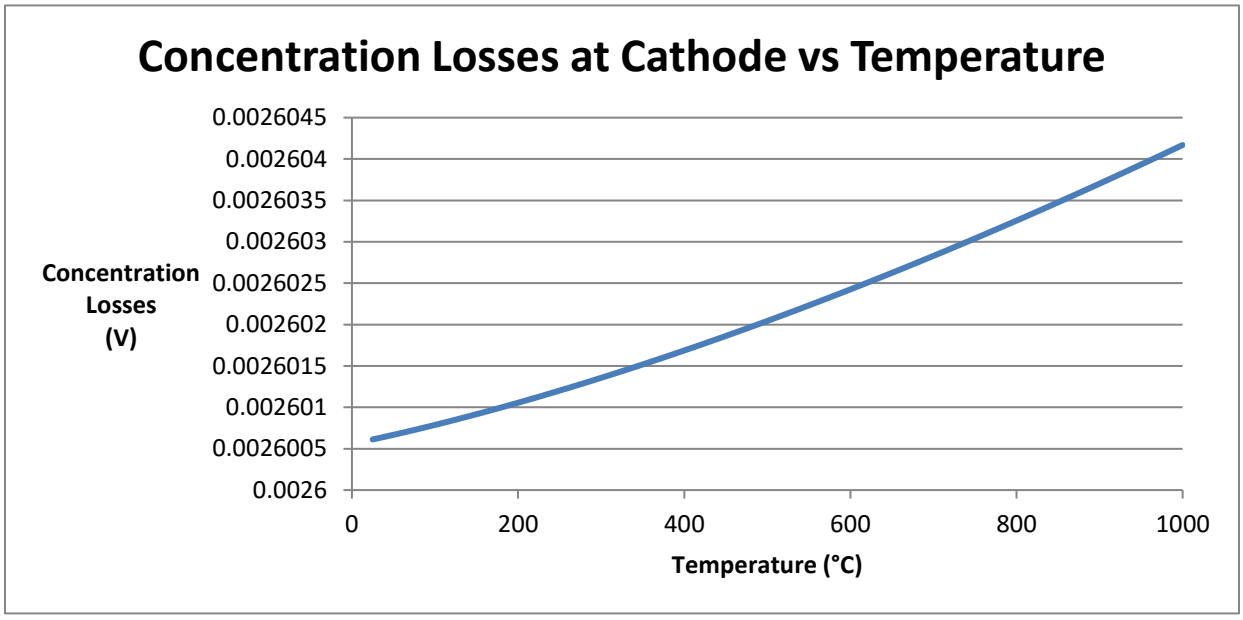

Figure 22. Graph Between Concentration Losses at Cathode and Temperature (Appendix 9)

Here, the concentration losses at cathode increase with the increase in the temperature. We have to choose an optimum temperature to minimize the concentration losses at cathode.

Effect of Current Density:

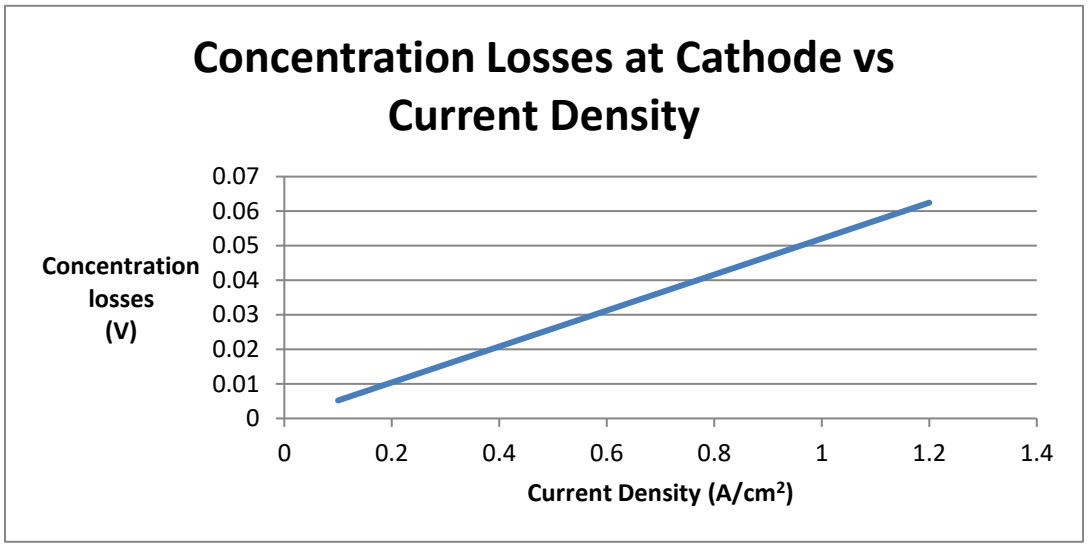

Figure 23. Graph Between Concentration Losses at Cathode and Current Density (Appendix 10)

Concentration losses are found to be directly proportional to current density.

Effect of Porosity:

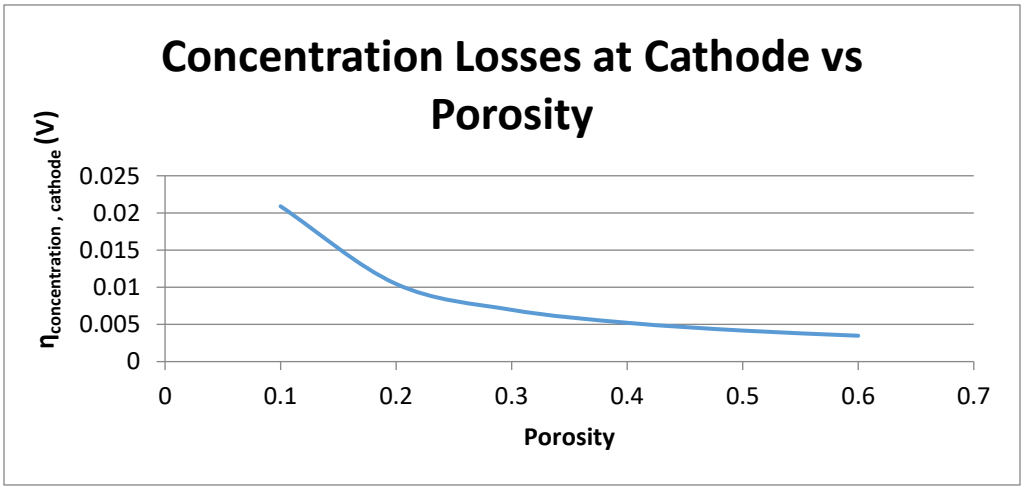

Figure 24. Graph Between Concentration Losses at Cathode and Porosity (Appendix 11)

When porosity increases, concentration over-potential at cathode decreases at an increasing rate.

Ohmic Losses:

It depends upon

1. Temperature
2. Current Density

Effect of Temperature:

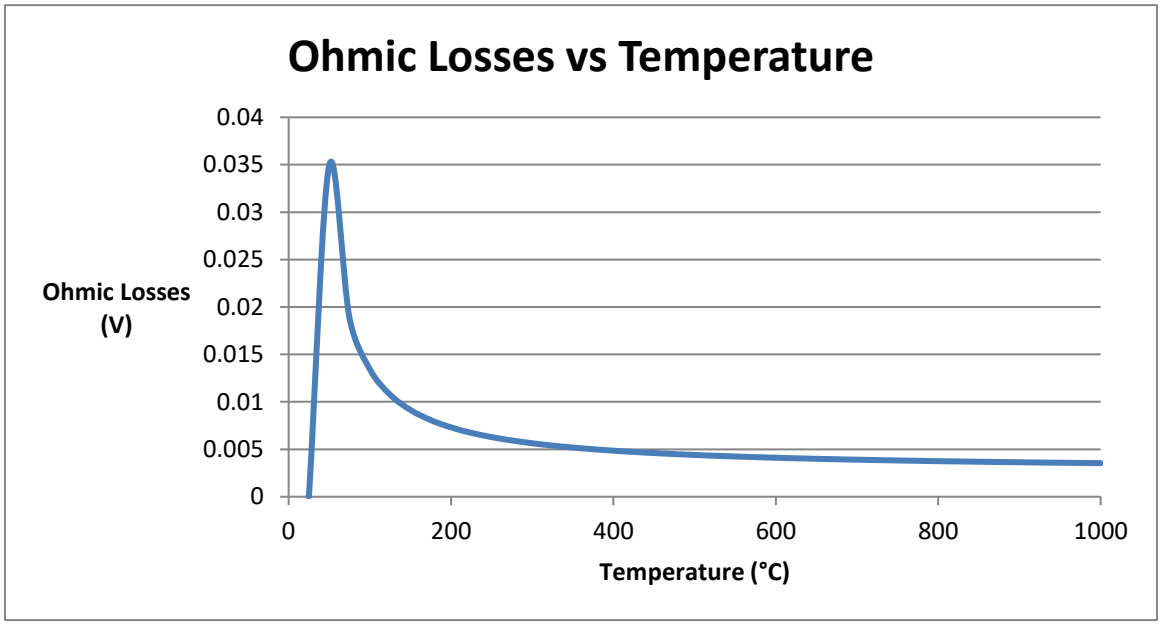

Figure 25. Graph Between Ohmic Losses and Temperature (Appendix 12)

Ohmic losses are maximum at a temperature of around 75 °C. At higher temperatures, Ohmic losses assume an approximate constant value.

Effect of Current Density:

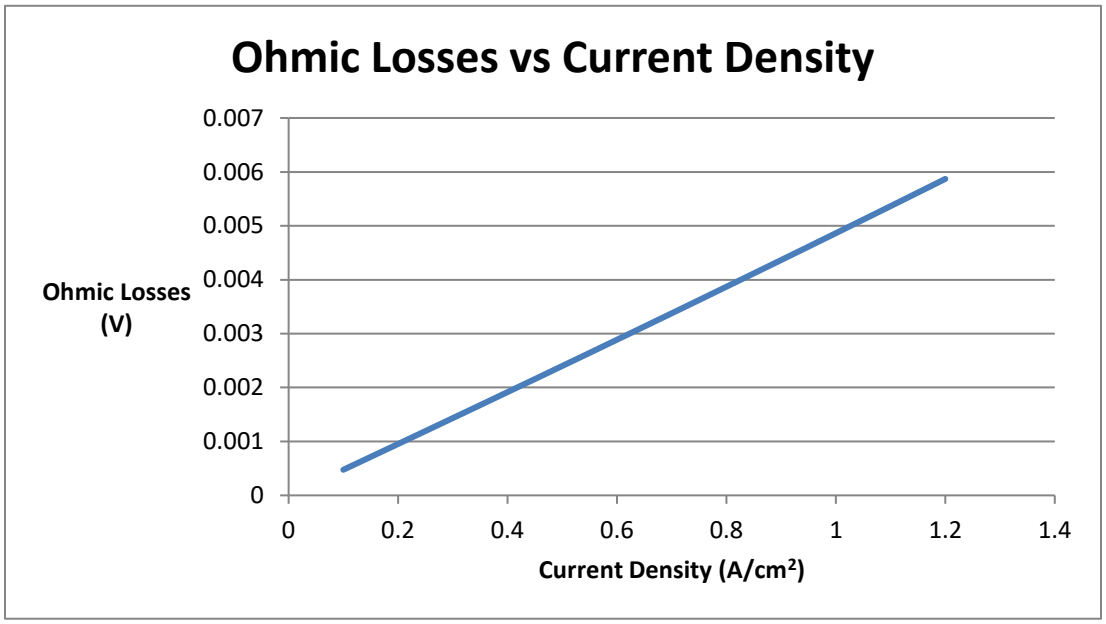

Figure 26. Graph Between Ohmic Losses and Current Density (Appendix 13)

Ohmic losses are directly proportional to the current density. Higher the current density, higher the ohmic losses.

Experimental and Theoretical Power Density:

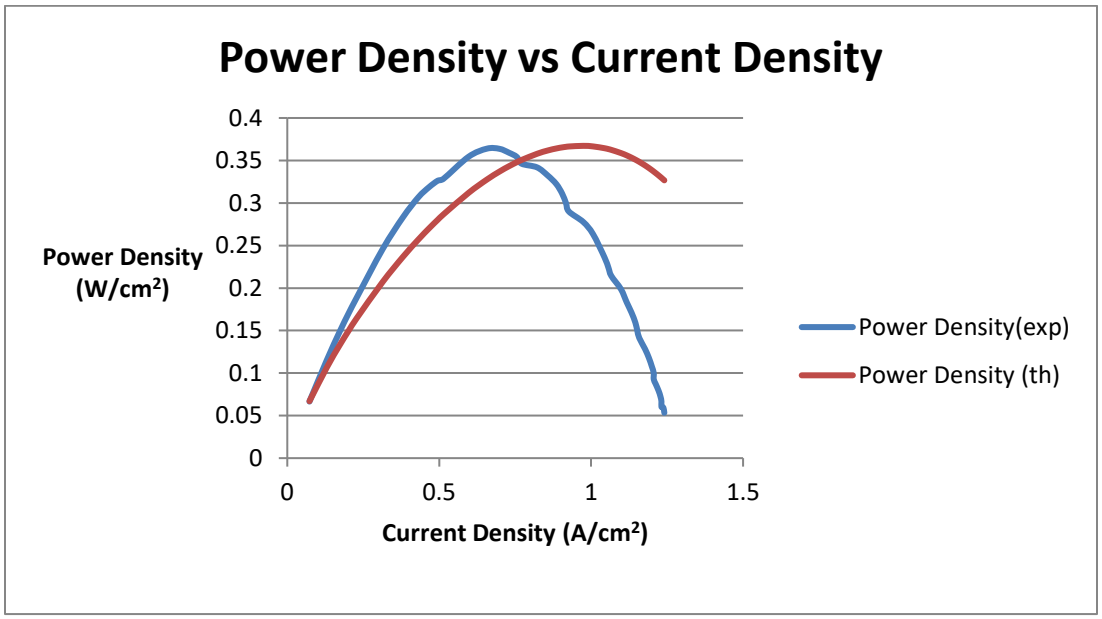

Figure 27. Graph Between Power Density and Current Density (Appendix 15)

Our theoretical solutions showed that the power density would have a maximum value of around 0.37 Wcm^{-2} when the current density is about 1 Acm^{-2}.

When the experiments were performed on our actual fuel cell, it was found that the maximum value that can be achieved for power density is still 0.37 W/cm^2 but at 0.7 Acm^{-2}.

The difference in the experimental and theoretical results could have been from physical world conditions from losses that were not accounted for during our analysis such as due impurities in the fuel used, or from internal currents.

For mehtane:

Methane shows similar trends as that by hydrogen. The final graph for methane is given as:

Total Voltage :

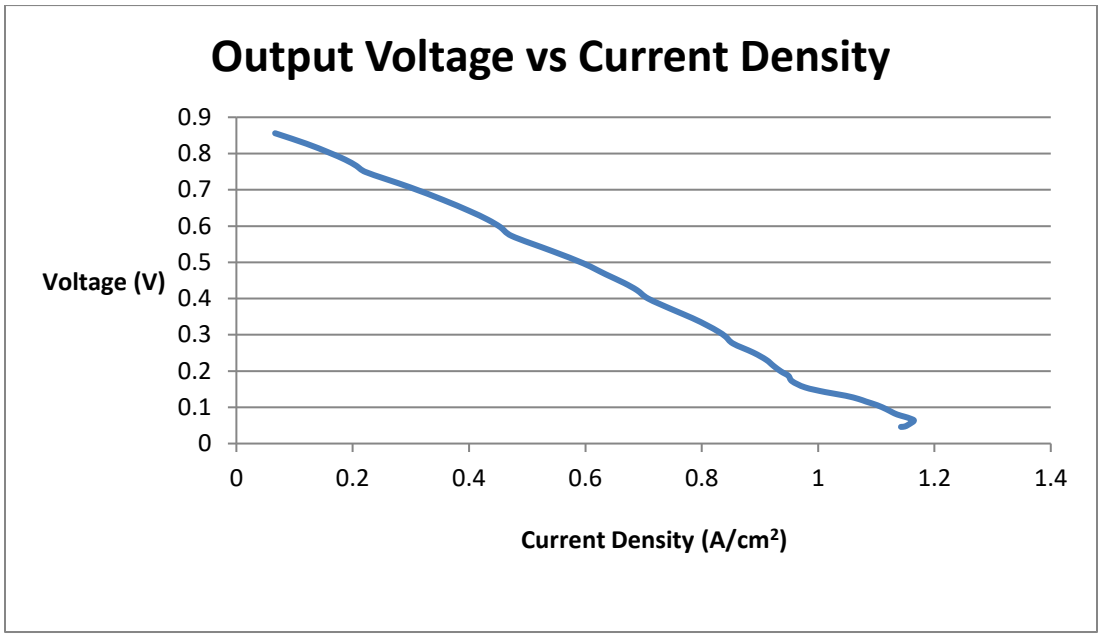

Figure 28. Graph Between Voltage and Current Density (Appendix 16)

Our experiments on the fuel cell, while using mathane as the fuel, showed that Voltage was seen to decrease at roughly a constant rate as the current density was increased.

Power Density:

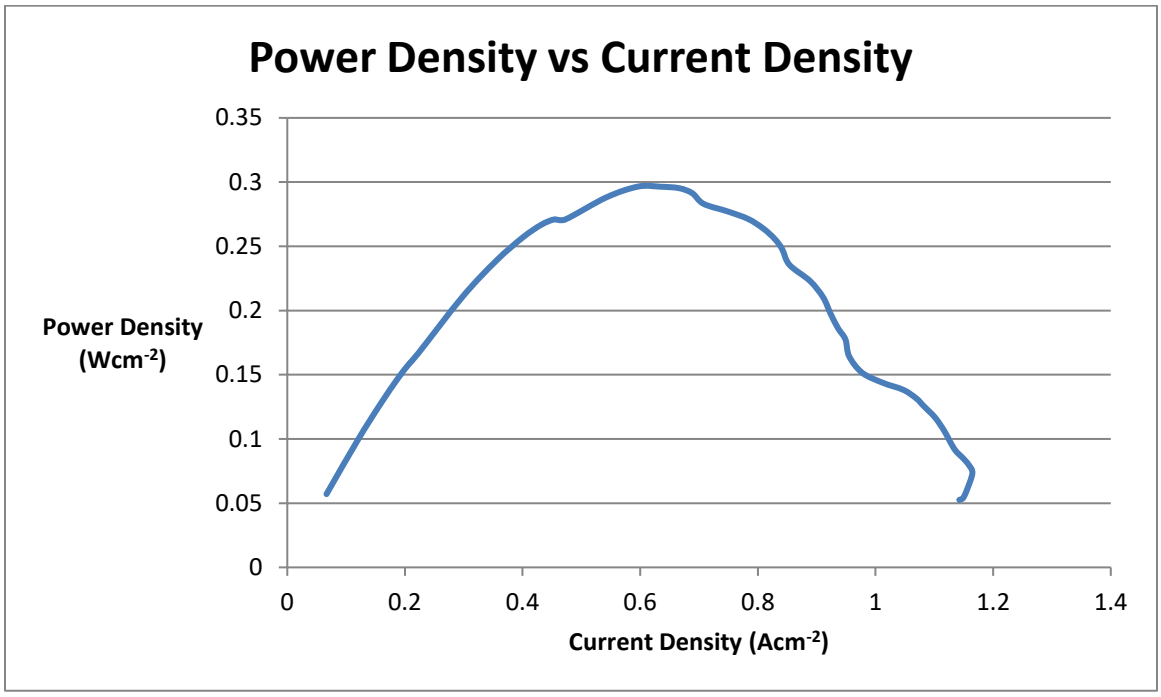

Figure 29. Graph Between Power Density and Current Density (Appendix 17)

A similar trend as that of Hydrogen was seen when methane was used as the fuel. Our experimental results show that the peak value of power density that was achieved was roughly 0.3 Wcm^{-2} when the current density is about 0.7 Acm^{-2}. This is very close to what we achieved with hydrogen.

Therefore, using methane as a fuel is also a very good alternative for. Since it's less explosive compared to hydrogen and it's also cheaper.

CFD Results

After the CFD was performed, most of our analytical results were verified. Figure 25 and Figure 26 shows how the mole fractions of Hydrogen and Oxygen vary along the single SOFC cell.

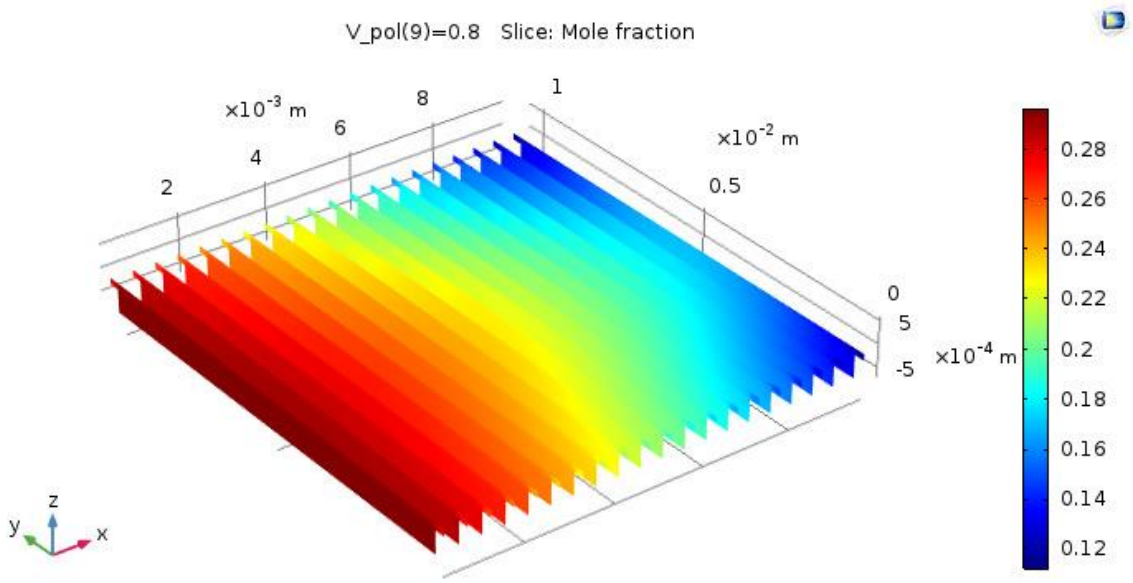

Figure 30. Hydrogen Mole Fraction Variation

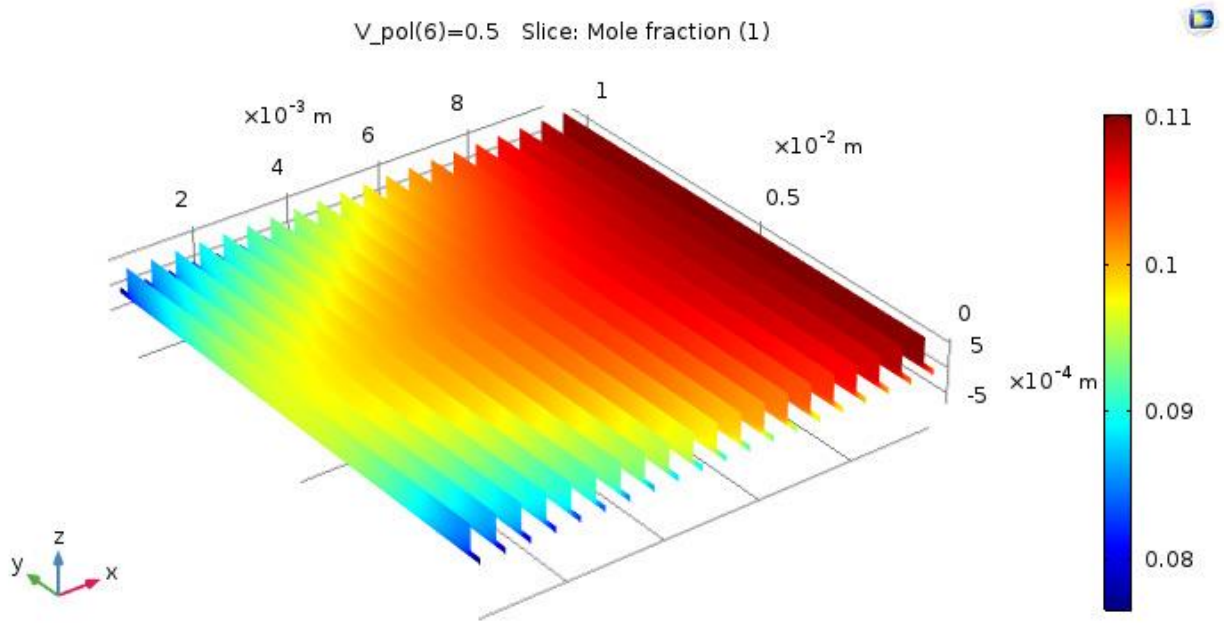

Figure 31. Mole Fraction of Oxygen

Next, the Figure 27 shows how the current density varies in the electrolyte at a polarization voltage of 0.5 V.

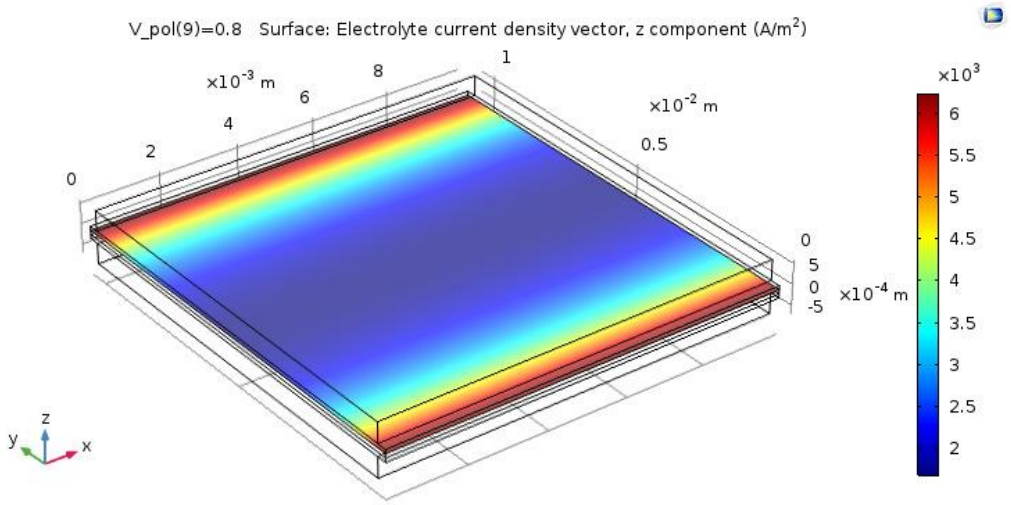

Figure 32. Electrolyte current density variation

Figure 32. shows how the polarization of voltage of the cell varies with the average current density.

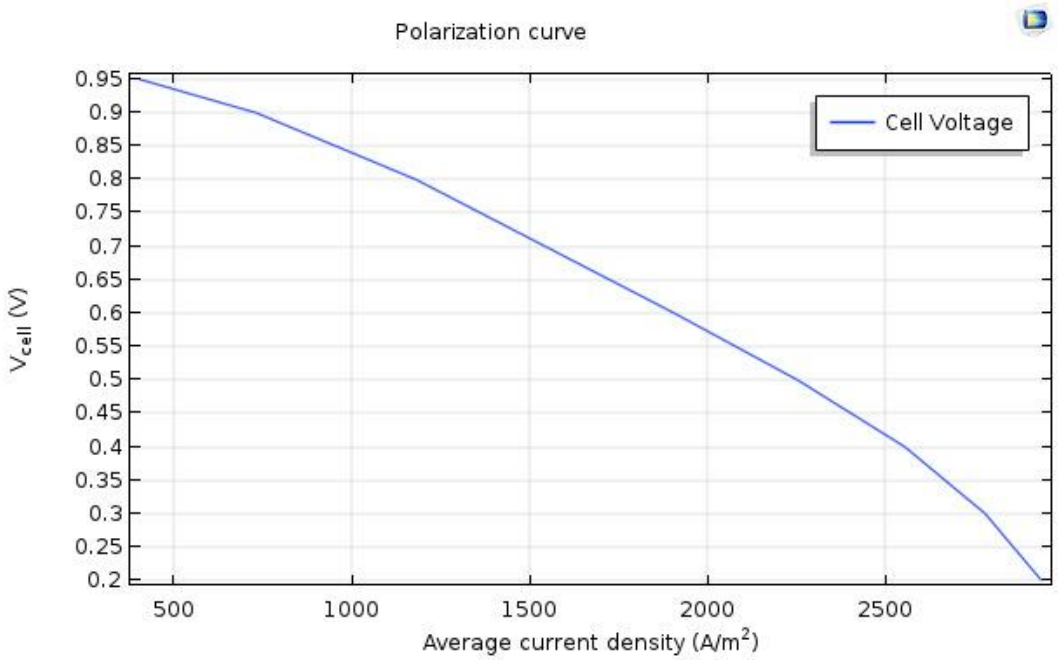

Figure 33. Polarization Curve

Finally, the total maximum output power was determined from the Power Vs Current curve. This came out to 1150 Wm^{-2} for our SOFC's Model.

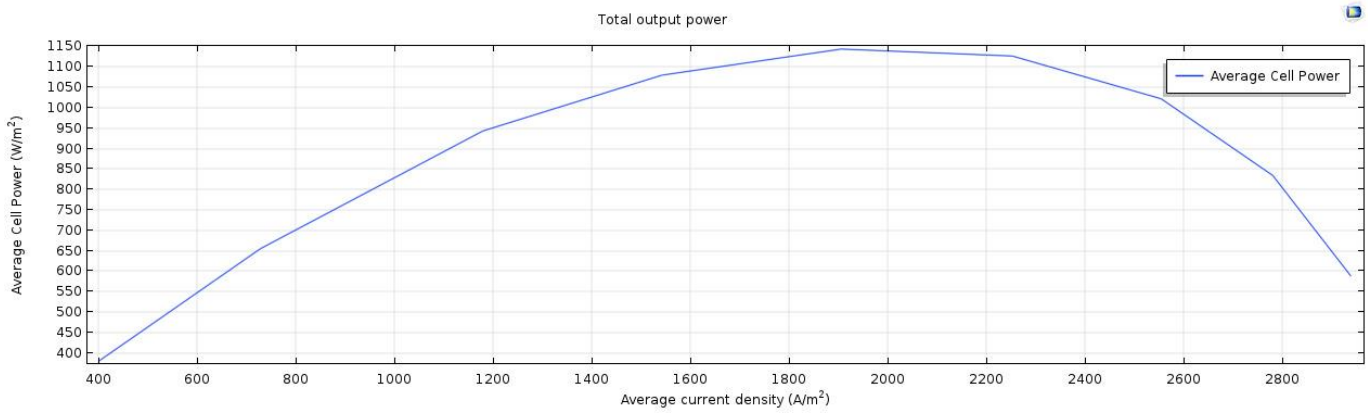

Figure 34. Power vs Current

CHAPTER 5: CONCLUSION AND RECOMMENDATION

Conclusion

From the material analysis, we were able to reach the following conclusions about the fuel cell:

- The configuration of the SOFC would be planar
- Area: 1 x 1 cm^2
- Anode: 500 nm thick Li-Ni-Cu-Zn
- Cathode: 20 μm thick Li-Ni-Cu-Zn
- Electrolyte: 150 μm thick La-Ba-CeO

From our analytical analysis and CFD analysis, we were able to conclude the parameters that our Solid Oxide Fuel Cell (SOFC) would be able to run on. From our analysis, these parameters would be able to give us optimum results. If these are incorporated into our project, a maximum power output of up to 0.354 Wcm^{-2} can be achieved neglecting any external losses such as concentration losses, activation losses, and Ohmic losses. These determined parameters were as following:

1. Temperature = 500-600 °C
2. Porosity = 0.4
3. Pore Radius = 3 μm
4. Current Density = 0.6-0.75 Acm^{-2}
5. P[H_2] = 3.45 atm

Recommendations

Another potential objective of our project is the implementation of the SOFC at the industries in Pakistan. A cogeneration plant as shown in Figure below can be executed to

Pakistani industries. Since burners in most industries run at temperatures of up to 1400K which is also the optimal temperature required for the fuel cell to work. A Reheater can be connected between the Fuel Cell and the burner that utilizes the carbon dioxide being released from the burner. This carbon dioxide is heated with coke in a forward boudouard reaction at 1000 k to produce Carbon Monoxide in a reversible reaction. Therefore, we have a supply of Carbon Monoxide for the inlet of the fuel cell. The advantages of this Cogeneration plant include increased efficiencies and reduced carbon emissions into the atmosphere and therefore, a reduction in global warming.

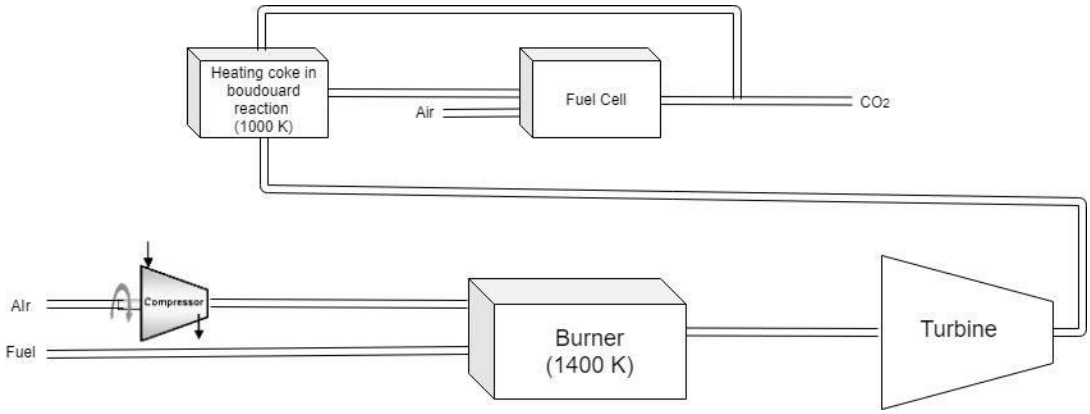

Figure 35. Flow chart depicting our Cogeneration plant implemented with a Steam Power plant

REFRENCES

1. Shafiee, S. and E. Topal, When will fossil fuel reserves be diminished? Energy Policy, 2009: p. 181-189.
2. Pakistan, M.o.P.a.N.R.-G.o., Coal Resources of Pakistan - An Overview. 2015
3. Ian Barnes, Upgrading the Efficiency of the World's Coal Fleet to Reduce CO2 Emissions. Cornerstone-The Official Journal of the World Coal Industry, 2015.
4. Giddey, S., Badwal, S.P.S; Kulkarni,A. & Munnings, C., Comprehensive review of direct carbon fuel cell technology. Progress in Energy and Combustion Science, 2012: p. 360-399.
5. Cao, D., Y. Sun, and G. Wang, Direct carbon fuel cell: Fundamentals and recent developments. Journal of Power Sources, 2007: p. 250-257.
6. Friedrich B. Prinz, Ryan P. O'Hayre, Suk Won Cha, and Whitney Colella; Fuel cell Fundamentals-3rd Edition Published by John Wiley & Sons, Inc., Hoboken, New Jersey
7. Blomen, L. JMJ, and M.N. Mugerwa, Fuel cell systems: History, in Springer Science & Business Media. 2013.
8. Dhathathreyan, K.S. and N. Rajalakshmi, Polymer Electrolyte Membrane Fuel Cell. Recent trends in fuel cell science and technology, 2007: p. 40-115.
9. Wang, Y., Ken Chen; Jeffrey Mishler; Sung Chan Cho & Xavier Cordobes Adroher, A review of polymer electrolyte membrane fuel cells: technology, applications, and needs on fundamental research. Applied energy, 2011. 88(4): p. 981-1007
10. Passalacqua, E.; Antonucci, P.L.; Vivaldi, M.; Patti, A. & Kinsoshita, K., The influence of Pt on the electrooxidation behavior of carbon in phosphoric acid. Electrochimica, 1992.
11. Hogarth, M.F. and G.A. Hards, Direct methanol fuel cells. Platinum Metals Review, 1996: p. 150-159.

12. Sammes, N., R. Bove, and K. Stahl, Phosphoricacid fuel cells: Fundamentals and applications. Current Opinion in Solid State and Materials Science, 2004: p. 372-378
13. McLean, G.F; Niet, T; Prince-Richard, S. & Djilali Ned, An assessment of alkaline fuel cell technology. International Journal of Hydrogen Energy 2002: p. 507-526.
14. Sotuchi, H., Energy Carriers And Conversion Systems. Alkaline Fuel Cells. 2.
15. Dicks, A.L., Molten carbonate fuel cells. Current Opinion in Solid State and Material Science, 2004: p. 379-383.
16. Plomp, L.; Veldhuis, J.B.J.; Sitters, E.F. & Vander Molen, S.B., Improvement of molten-carbonate fuel cell (MCFC) lifetime. Journal of power sources, 1992: p. 369-373
17. Ormerod, R.M., Solid oxide fuel cells. Chemical Society Reviews, 2003: p. 17-28.
18. Hernandez-Racheco E, Singh D, Hutton PN, Patel N, Mann MD. A macro-level model for determining the performance characteristics of solid oxide fuel cells. J Power Sources 2004;138(1–2):174–86.
19. Chan SH, Khor KA, Xia ZT. A complete polarization model of a solid oxide fuel cell and its sensitivity to the change of component thickness. J Power Sources 2001;93(1–2):130–40.
20. Chan SH, Xia ZT. Polarization effects in electrolyte/electrodesupported solid oxide fuel cells. J Appl Electrochem 2002;32(3): 339–47.
21. Song TW, Sohn JL, Kim JH, Kim TS, Ro ST, Suzuki K. Performance analysis of a tubular solid oxide fuel cell/micro gas turbine hybrid power system based on a quasi-two dimensional model. J Power Sources 2005;142(1–2):30–42.
22. Song TW, Sohn JL, Kim JH, Kim TS, Ro ST, Suzuki K. Performance analysis of a tubular solid oxide fuel cell/micro gas turbine hybrid

power system based on a quasi-two dimensional model. J Power Sources 2005;142(1–2):30–42.

23. Petruzzi L, Cocchi S, Fineschi F. A global thermo-electrochemical model for SOFC system design and engineering. J Power Sources 2003;118(1–2):96–107.
24. Petruzzi L, Cocchi S, Fineschi F. A global thermo-electrochemical model for SOFC system design and engineering. J Power Sources 2003;118(1–2):96–107.
25. M Ni, MKH Leung, DYC Leung - Energy Conversion and Management, 2007 – Elsevier
26. Lu YX, Schaefer L, Li PW. Numerical study of a flat-tube high power density solid oxide fuel cell – part 1. heat/mass transfer and fluid flow. J Power Sources 2005;140(2):331–9.
27. Khaleel MA, Lin Z, Singh P, Surdoval W, Collin D. A finite element analysis modeling tool for solid oxide fuel cell development: coupled electrochemistry, thermal and flow analysis in MARC(R). J Power Sources 2004;130(1–2):136–48.
28. Xue X, Tang J, Sammes N, Du Y. Dynamic modeling of single tubular SOFC combining heat/mass transfer and electrochemical reaction effects. J Power Sources 2005;142(1–2):211–22.
29. The Engineering Tool Box, Standard State enthalpy formation Gibbs Free Energy; Published on 2017, Retrieved from: <https://www.engineeringtoolbox.com/standard-state-enthalpy-formation-definition-value-Gibbs-free-energy-entropy-molar-heat-capacity-d_1978.html>
30. Chan SH, Khor KA, Xia ZT. A complete polarization model of a solid oxide fuel cell and its sensitivity to the change of component thickness. J Power Sources 2001;93(1–2):130–40.
31. Chan SH, Xia ZT. Polarization effects in electrolyte/electrodesupported solid oxide fuel cells. J Appl Electrochem 2002;32(3):339–47.

32. Ni M, Leung MKH, Leung DYC. An electrochemical model of a solid oxide steam electrolyzer for hydrogen production. Chem Eng Technol 2006;29(5):636–42.
33. Barbir F. PEM fuel cells-theory and practice. Elsevier Academic Press; 2005. pp. 36–39.
34. Hernandez-Pacheco E, Mann MD, Hutton PN, Singh D, Martin KE. A cell-level model for a solid oxide fuel cell operated with syngas from a gasification process. Int J Hydrogen Energy 2005;30(11):1221–33.
35. Costamagna P, Honegger K. Modeling at solid oxide heat exchanger integrated stacks and simulation at high fuel utilization. J Electrochem Soc 1998;145(11):3995–4007.
36. Costamagna P, Selimovic A, Borghi MD, Agnew G. Electrochemical model of the integrated planar solid oxide fuel cell (IP-SOFC). Chem Eng J 2004;102(1):61–9.
37. Calise F, Palombo A, Vanoli L. Design and partial load exergy analysis of hybrid SOFC–GT power plant, J. Power Sources, doi:10.1016/j.jpowsour.2005.07.088.
38. Deng XH, Petric A. Geometrical modeling of the triple-phaseboundary in solid oxide fuel cells. J Power Sources 2005;140(2):297–303
39. Hernandez-Racheco E, Singh D, Hutton PN, Patel N, Mann MD. A macro-level model for determining the performance characteristics of solid oxide fuel cells. J Power Sources 2004;138(1–2):174–86.
40. Reid RC, Prausnitz JM, Polling BE. The properties of gases and liquids. 4th ed. McGraw-Hill Book Company; 1987, ISBN 0-07-051799-1.
41. Suwanwarangkul R, Croiset E, Fowler MW, Douglas PL, Entchev E, Douglas MA. Performance comparison of Fick's, dusty gas and Stefan Maxwell models to predict the concentration overpotential of a SOFC anode. J Power Sources 2003;122(1):9–18.
42. Ferguson JR, Fiard JM, Herbin R. Three-dimensional numerical simulation for various geometries of solid oxide fuel cells. J Power Sources 1996;58(2):109–22.

43. Fuel Cell Materials, Scandia Stabilized Zirconia; Retrieved from: <https://fuelcellmaterials.com/products/powders/electrolyte-powders/scandia-stabilized-zirconia-10-sc-powder/>

APPENDICES

APPENDIX 1: EQUIVALENT VOLTAGE VS TEMPERATURE

Temperature(°C)	Equivalent Voltage (V)
25	1.190533
50	1.185228
75	1.179823
100	1.174322
125	1.168732
150	1.163058
175	1.157308
200	1.151488
225	1.145602
250	1.139657
275	1.133659
300	1.127611
325	1.121518
350	1.115386
375	1.109217
400	1.103015
425	1.096784
450	1.090528

475	1.084248
500	1.077948
525	1.07163
550	1.065297
575	1.058951
600	1.052594
625	1.046228
650	1.039855
675	1.033476
700	1.027094
725	1.02071
750	1.014325
775	1.00794
800	1.001557
825	0.995178
850	0.988802
875	0.982432
900	0.976068
925	0.969711
950	0.963362
975	0.957022
1000	0.950692

APPENDIX 2: EQUIVALENT VOLTAGE VS PRESSURE OF HYDROGEN GAS

Pressure of Hydrogen Gas (atm)	Equivalent Voltage (V)
0.098692	0.939232
0.197385	0.96381
0.296077	0.978187
0.394769	0.988388
0.493462	0.9963
0.592154	1.002765
0.690846	1.008231
0.789539	1.012966
0.888231	1.017142
0.986923	1.020878
1.085616	1.024258
1.184308	1.027343
1.283	1.030181
1.381693	1.032809
1.480385	1.035255
1.579077	1.037544
1.67777	1.039693
1.776462	1.04172
1.875154	1.043637
1.973847	1.045456

2.072539	1.047186
2.171231	1.048836
2.269924	1.050412
2.368616	1.051921
2.467308	1.053368
2.566	1.054759
2.664693	1.056097
2.763385	1.057387
2.862077	1.058631
2.96077	1.059833
3.059462	1.060996
3.158154	1.062122
3.256847	1.063213
3.355539	1.064271
3.454231	1.065299
3.552924	1.066298
3.651616	1.06727
3.750308	1.068215
3.849001	1.069136
3.947693	1.070034
4.046385	1.070909
4.145078	1.071764

4.24377	1.072598
4.342462	1.073413
4.441155	1.07421
4.539847	1.07499
4.638539	1.075752
4.737232	1.076499
4.835924	1.07723
4.934616	1.077946

APPENDIX 3: EQUIVALENT VOLTAGE VS TEMPERATURE

Temperature (°C)	Activation Losses (V)
25	0.634336
50	0.607593
75	0.58085
100	0.554108
125	0.527365
150	0.500622
175	0.473879
200	0.447136
225	0.420393

250	0.39365
275	0.366908
300	0.340165
325	0.313422
350	0.286679
375	0.259936
400	0.233193
425	0.20645
450	0.179708
475	0.152965
500	0.126222
525	0.099479
550	0.072736
575	0.045993
600	0.019251

APPENDIX 4: ACTIVATION LOSSES VS CURRENT DENSITY

Current Density (Acm^{-2})	Activation Losses (V)
0.025	0
0.05	0.072736
0.075	0.13714
0.1	0.182835
0.125	0.218279
0.15	0.247239
0.175	0.271724
0.2	0.292934
0.225	0.311642
0.25	0.328378
0.275	0.343517
0.3	0.357338
0.325	0.370052
0.35	0.381823
0.375	0.392782
0.4	0.403033
0.425	0.412662
0.45	0.421741
0.475	0.430329
0.5	0.438477

0.525	0.446226
0.55	0.453616
0.575	0.460676
0.6	0.467436
0.625	0.473921
0.65	0.48015
0.675	0.486145
0.7	0.491922
0.725	0.497495
0.75	0.50288
0.775	0.508089
0.8	0.513132
0.825	0.518019
0.85	0.522761
0.875	0.527365
0.9	0.53184
0.925	0.536192
0.95	0.540428
0.975	0.544554
1	0.548575
1.025	0.552498
1.05	0.556325

1.075	0.560063
1.1	0.563714
1.125	0.567284
1.15	0.570775
1.175	0.574191
1.2	0.577535
1.225	0.58081
1.25	0.584019

APPENDIX 5: ACTIVATION LOSSES VS POROSITY

Porosity	**Activation Losses (V)**
0.1	0.04433857
0.2	0.027646803
0.3	0.023567508
0.4	0.024285356
0.5	0.030836038
0.6	0.060521534

APPENDIX 6: ACTIVATION LOSSES VS PORE SIZE

Pore Size (10^{-5} m)	Activation Losses (V)
0.1	0.000001
0.2	0.35
0.3	0.28
0.4	0.29
0.5	0.36
0.6	0.42

APPENDIX 7: CONCENTRATION LOSSES AT ANODE VS TEMPERATURE

Temperature (°C)	Concentration Losses at Anode (V)
25	5.9195E-07
50	6.2119E-07
75	6.5158E-07
100	6.8308E-07
125	7.1565E-07
150	7.4927E-07
175	7.8389E-07
200	8.195E-07
225	8.5606E-07

250	8.9355E-07
275	9.3194E-07
300	9.7122E-07
325	1.0114E-06
350	1.0524E-06
375	1.0942E-06
400	1.1368E-06
425	1.1803E-06
450	1.2245E-06
475	1.2695E-06
500	1.3153E-06
525	1.3618E-06
550	1.409E-06
575	1.457E-06
600	1.5056E-06
625	1.555E-06
650	1.6051E-06
675	1.6558E-06
700	1.7072E-06
725	1.7593E-06
750	1.8121E-06
775	1.8655E-06

800	1.9195E-06
825	1.9742E-06
850	2.0295E-06
875	2.0854E-06
900	2.1419E-06
925	2.199E-06
950	2.2567E-06
975	2.3151E-06
1000	2.374E-06

APPENDIX 8: CONCENTRATION LOSSES AT ANODE VS POROSITY

Porosity	Concentration Losses at Anode (V)
0.1	6.99161E-05
0.2	3.49632E-05
0.3	2.33099E-05
0.4	1.74829E-05
0.5	1.39865E-05
0.6	1.16555E-05

APPENDIX 9: CONCENTRATION LOSSES AT CATHODE VS TEMPERATURE

Temperature (°C)	Concentration Losses at Cathode (V)
25	0.00260061
50	0.00260067
75	0.00260073
100	0.00260079
125	0.00260085
150	0.00260092
175	0.00260099
200	0.00260106
225	0.00260113
250	0.0026012
275	0.00260128
300	0.00260136
325	0.00260144
350	0.00260152
375	0.0026016
400	0.00260169
425	0.00260177
450	0.00260186
475	0.00260195
500	0.00260204

525	0.00260214
550	0.00260223
575	0.00260233
600	0.00260242
625	0.00260252
650	0.00260262
675	0.00260273
700	0.00260283
725	0.00260293
750	0.00260304
775	0.00260315
800	0.00260326
825	0.00260337
850	0.00260348
875	0.00260359
900	0.0026037
925	0.00260382
950	0.00260393
975	0.00260405
1000	0.00260417

APPENDIX 10: CONCENTRATION LOSSES AT CATHODE VS CURRENT DENSITY

Current Density (Acm^{-2})	Concentration Losses at Cathode (V)
0.1	0.005204
0.2	0.010409
0.3	0.015614
0.4	0.020819
0.5	0.026023
0.6	0.031228
0.7	0.036433
0.8	0.041638
0.9	0.046843
1	0.052048
1.1	0.057253
1.2	0.062457

APPENDIX 11: CONCENTRATION LOSSES AT CATHODE VS POROSITY

Porosity	Concentration Losses at Cathode (V)
0.1	0.020897
0.2	0.010448
0.3	0.006964
0.4	0.005223

0.5	0.004178
0.6	0.003481

APPENDIX 12: OHMIC LOSSES VS TEMPERATURE

Temperature (°C)	Ohmic Losses (V)
25	Not defined
50	0.034922
75	0.018813
100	0.013443
125	0.010758
150	0.009148
175	0.008074
200	0.007307
225	0.006732
250	0.006284
275	0.005927
300	0.005634
325	0.00539

350	0.005184
375	0.005007
400	0.004853
425	0.004719
450	0.004601
475	0.004496
500	0.004402
525	0.004317
550	0.004241
575	0.004171
600	0.004108
625	0.00405
650	0.003996
675	0.003947
700	0.003901
725	0.003859
750	0.00382
775	0.003783
800	0.003748
825	0.003716
850	0.003686
875	0.003657

900	0.003631
925	0.003605
950	0.003582
975	0.003559
1000	0.003537

APPENDIX 13: OHMIC LOSSES VS CURRENT DENSITY

Current Density (Acm^{-2})	Ohmic Losses (V)
0.1	0.000475
0.2	0.000953
0.3	0.001433
0.4	0.001915
0.5	0.0024
0.6	0.002887
0.7	0.003377
0.8	0.00387
0.9	0.004365
1	0.004864
1.1	0.005365
1.2	0.00587

APPENDIX 14: EXPERIMENTAL AND THEORETICAL OUTPUT VOLTAGE WITH HYDROGEN AS FUEL VS CURRENT DENSITY

Current Density (Acm^{-2})	Output Voltage Experimental (V)	Output Voltage Theoretical (V)
0.072993	0.912	0.917341
0.130118	0.886	0.819685
0.171375	0.863	0.771657
0.203111	0.843	0.741331
0.2285	0.826	0.719918
0.314187	0.783	0.659952
0.380833	0.744	0.621765
0.43161	0.711	0.595827
0.46652	0.683	0.579167
0.495082	0.659	0.56611
0.514124	0.639	0.557651
0.596638	0.594	0.522794
0.656936	0.554	0.498674
0.698193	0.521	0.482603
0.729929	0.492	0.470405
0.755318	0.469	0.460716
0.771186	0.449	0.454683
0.821964	0.416	0.435431

0.856874	0.388	0.422185
0.885436	0.364	0.411305
0.904478	0.344	0.404018
0.917172	0.327	0.399141
0.926693	0.313	0.395471
0.974297	0.285	0.376943
1.006033	0.262	0.364388
1.044116	0.226	0.349058
1.056811	0.212	0.343875
1.066332	0.201	0.339961
1.098068	0.181	0.326746
1.117109	0.164	0.31868
1.132977	0.151	0.311875
1.145672	0.139	0.306372
1.152019	0.13	0.303601
1.158366	0.122	0.300816
1.177408	0.109	0.292377
1.190102	0.099	0.286677
1.199623	0.09	0.282363
1.20597	0.083	0.279467
1.20597	0.077	0.279467
1.212317	0.072	0.276555

1.221838	0.065	0.272157
1.228185	0.059	0.269204
1.231359	0.054	0.267722
1.231359	0.049	0.267722
1.237706	0.048	0.264744
1.24088	0.043	0.263248

APPENDIX 15: EXPERIMENTAL AND THEORETICAL POWER DENSITY WITH HYDROGEN AS FUEL VS CURRENT DENSITY

Current Density (Acm^{-2})	**Power Density Experimental (Wcm^{-2})**	**Power Density Theoretical (Wcm^{-2})**
0.072993	0.06657	0.066959
0.130118	0.115284	0.106656
0.171375	0.147896	0.132243
0.203111	0.171222	0.150572
0.2285	0.188741	0.164501
0.314187	0.246008	0.207348
0.380833	0.28334	0.236789
0.43161	0.306875	0.257165

0.46652	0.318633	0.270193
0.495082	0.326259	0.280271
0.514124	0.328525	0.286702
0.596638	0.354403	0.311919
0.656936	0.363943	0.327597
0.698193	0.363759	0.33695
0.729929	0.359125	0.343362
0.755318	0.354244	0.347987
0.771186	0.346263	0.350646
0.821964	0.341937	0.357908
0.856874	0.332467	0.361759
0.885436	0.322299	0.364185
0.904478	0.31114	0.365425
0.917172	0.299915	0.366081
0.926693	0.290055	0.36648
0.974297	0.277675	0.367254
1.006033	0.263581	0.366586
1.044116	0.23597	0.364457
1.056811	0.224044	0.36341
1.066332	0.214333	0.362512
1.098068	0.19875	0.358789
1.117109	0.183206	0.356001

1.132977	0.17108	0.353347
1.145672	0.159248	0.351002
1.152019	0.149762	0.349754
1.158366	0.141321	0.348455
1.177408	0.128337	0.344246
1.190102	0.11782	0.341175
1.199623	0.107966	0.338729
1.20597	0.100096	0.337029
1.20597	0.09286	0.337029
1.212317	0.087287	0.335273
1.221838	0.079419	0.332532
1.228185	0.072463	0.330633
1.231359	0.066493	0.329661
1.231359	0.060337	0.329661
1.237706	0.05941	0.327675
1.24088	0.053358	0.326659

APPENDIX 16: EXPERIMENTAL OUTPUT VOLTAGE USING METHANE AS FUEL VS CURRENT DENSITY

Current Density (Acm^{-2})	Experimental Output Voltage (V)
0.066646	0.856
0.120597	0.827
0.15868	0.803
0.187243	0.783
0.206284	0.766
0.222152	0.749
0.298319	0.707
0.355444	0.672
0.399874	0.642
0.43161	0.618
0.453826	0.597
0.472867	0.573
0.542687	0.531
0.596638	0.497
0.634721	0.467
0.666457	0.443
0.688672	0.423
0.707714	0.4

0.748971	0.37
0.783881	0.346
0.809269	0.326
0.828311	0.309
0.841006	0.295
0.8537	0.276
0.88861	0.251
0.910825	0.231
0.923519	0.214
0.936214	0.199
0.948908	0.187
0.955255	0.172
0.977471	0.155
1.01238	0.142
1.04729	0.132
1.069505	0.123
1.0822	0.116
1.101241	0.106
1.117109	0.095
1.12663	0.087
1.136151	0.08
1.148845	0.074

1.158366	0.069
1.164713	0.063
1.155192	0.052
1.148845	0.047
1.142498	0.046

APPENDIX 17: EXPERIMENTAL POWER DENSITY USING METHANE AS FUEL VS CURRENT DENSITY

Current Density (Acm^{-2})	Experimental Power Density (Wcm^{-2})
0.021	0.066646
0.038	0.120597
0.05	0.15868
0.059	0.187243
0.065	0.206284
0.07	0.222152
0.094	0.298319
0.112	0.355444
0.126	0.399874
0.136	0.43161
0.143	0.453826
0.149	0.472867

0.171	0.542687
0.188	0.596638
0.2	0.634721
0.21	0.666457
0.217	0.688672
0.223	0.707714
0.236	0.748971
0.247	0.783881
0.255	0.809269
0.261	0.828311
0.265	0.841006
0.269	0.8537
0.28	0.88861
0.287	0.910825
0.291	0.923519
0.295	0.936214
0.299	0.948908
0.301	0.955255
0.308	0.977471
0.319	1.01238
0.33	1.04729
0.337	1.069505

0.341	1.0822
0.347	1.101241
0.352	1.117109
0.355	1.12663
0.358	1.136151
0.362	1.148845
0.365	1.158366
0.367	1.164713
0.364	1.155192
0.362	1.148845
0.36	1.142498

APPENDIX 18: MOLECULAR DIFFUSION COEFFICIENT

Substance	σ (Å)	ε_{AB}/kb (K)
O_2	3.467	106.7
CO	3.690	91.7
CO_2	3.941	195.2

K_BT/ ε_{12}	Ω	K_BT/ ε_{12}	Ω
0.30	2.662	2.5	0.9996
0.40	2.318	2.7	0.9770
0.50	2.066	2.9	0.9576
0.60	1.877	3.3	0.9256
0.70	1.729	3.7	0.8998
0.80	1.612	3.9	0.8888
0.90	1.517	4.0	0.8836
1.00	1.439	4.2	0.8740
1.10	1.375	4.4	0.8652
1.30	1.273	4.6	0.8568
1.50	1.198	4.8	0.8492
1.60	1.167	5.0	0.8422
1.65	1.153	7	0.7896
1.75	1.128	9	0.7556
1.85	1.105	20	0.6640
1.95	1.084	60	0.5596
2.1	1.057	100	0.5130
2.3	1.026	300	0.4360